ISSP International Workshop and Symposium: Foundation and Application of DFT
August 8, 2007

Molecular Theory For Large Systems

T.Tsuneda, T. Nakajima, and K. Hirao
The University of Tokyo

東京大学
THE UNIVERSITY OF TOKYO

UT Research Activities

Ab initio Theory

MRMP, MCQDPT
CASVB, QCAS, SPS-SCF&PT
Linear Scaling Method
(PS, RI, Local MP2, Plane wa

DFT

OP Correlation
Parameter-Free Exchange
Long-range corrected functional
TDDFT
Dual-level DFT

UTChem

Relativistic Theory

RESC, DK3
Dirac-Hartree-Fock
Dirac-Kohn-Sham
Ab initio Model Potential
Relativistic Basis Sets

Dynamics

Ab initio dynamics
(TD)DFT dynamics
Hybrid QM/MM
VSCF,VCI

UTChem A Program Suite for ab initio Quantum Chemistry

Ab initio MO, DFT, and Dynamics

Non-relativistic and Relativistic
(Two- and Four-component relativistic)

CISD, CISDT, CISDTQ,
CCSD, CCSDT, CCSDTQ,
MP2, MP3, and MP4,

are implemented into UTChem.

Limitted to developers

Login
Information

http://utchem.qcl.t.u-tokyo.ac.jp/

Copyright © 2002, 2003, 2004 UTChem developers group. All right reserved.

Two Approaches to Molecular Theory

- **Wave Function Method**

  Huge and successful efforts in the last 30 years

  State-of-the-art methodology

  Systematic, Converging to exact solution

  Accurate results for small systems

  Steep N dependence of the computational effort

- **Density Method (Density Functional Theory)**

  Not reached such a mature stage as wave function method

  Not *ab initio*, but best semi-empirical

  Simple and conceptual, Applicable to large systems

  Accuracy depends on *xc* functionals

Spectroscopic Constants of Diatomic Hydrides

Main-group elements across the second- through fifth-period of the periodic table

J.Chem.Phys. **120**, 3297 (2004)

BH	CH	NH	OH	FH
AlH	SiH	PH	SH	ClH
GaH	GeH	AsH	SeH	BrH
InH	SnH	SbH	TeH	IH

DK3-CCSD, DK3-CCSDT, DK3-CCSDTQ

Re-contracted relativistic cc-pVnZ (n=2-5)

Extrapolation

DK3 is the third-order Douglas-Kroll approximation.

Spectroscopic Constants of CH and InH

	^{12}CH ($^2\Pi$)		^{115}InH($^1\Sigma^+$)	
	Theory	**Exp.**	**Theory**	**Exp.**
r_e / Å	1.120	1.120	1.841	1.838
r_0 / Å	1.131	1.130	1.855	1.851
B_e / cm^{-1}	14.449	14.457	4.977	4.995
B_0 / cm^{-1}	14.182	14.190	4.905	4.923
α_e / cm^{-1}	0.534	0.534	0.144	0.143
D_e / cm^{-1}	0.00148	0.00145	0.000229	0.000223
ω_e / cm^{-1}	2860	2859	1467	1476
$x\omega_e$ / cm^{-1}	66	63	26	26
ν_0 / cm^{-1}	1413	1413	727	732
ν_1 / cm^{-1}	4141	4146	2142	2157
ν_2 / cm^{-1}	6743	6752	3510	3535
D_0^0 / eV	3.47	3.47	2.46	2.48

Theory (DK3-CC) can predict the experimental

Bond lengths (r_e or r_0) within 0.002 Å
Rotational constants (B_e or B_0) within 0.02 cm^{-1}
Vibration-rotation constants (α_e) within 0.01 cm^{-1}
Centrifugal distortion constants (D_e) within 2 %
Harmonic vibrational constants (ω_e) within 9 cm^{-1}
Anharmonic vibrational constants ($\chi\omega_e$) within 2 cm^{-1}
Dissociation energies (D_0^0) within 0.02 eV (0.4 kcal/mol)

The theoretical best estimate will substitute for the missing experimental data for some fourth- and fifth-row hydrides.

Spectroscopic constants of the $^2\Pi$ state of ^{130}TeH

	Theory	Exptl.
r_e / Å	1.656	1.656[a]
r_0 / Å	1.667	1.741[b]
B_e / cm^{-1}	6.149	
B_0 / cm^{-1}	6.067	5.56[b]
α_e / cm^{-1}	0.165	
D_e / cm^{-1}	0.000200	
ω_e / cm^{-1}	2144	(2137)[a]
$x\omega_e$ / cm^{-1}	39	
ν_0 / cm^{-1}	1062	
ν_1 / cm^{-1}	3128	
ν_2 / cm^{-1}	5119	
D_0^0 / eV	2.76	

Fermi Resonance of CO_2

Yagi et al, J.Chem.Phys. **126**, 124303 (2007)

A characterization of the spectroscopic properties of CO_2 is crucial for the understanding of chemistry of the seafloor, planetary atmospheres, and the greenhouse effect.

CO_2 has four normal modes of vibrations:

(a) a symmetric stretching mode (ν_1),

(b) degenerate bending modes (ν_2)

(c) an antisymmetric stretching mode (ν_3).

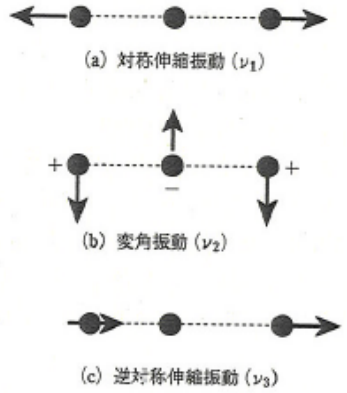

The accidental near degeneracy, $\nu_1 \approx 2\nu_2$, results in a significant anharmonic coupling between the two modes, which are pushed apart by the coupling. This is the well known ν_1-$2\nu_2$ Fermi resonance of CO_2.

Low-lying vibrational energy levels (in cm^{-1}) of CO_2 obtained with CCSD(T) and vibrational CI

	Theory	Exptl.	
ν_2 (01^10)	668.5	667.4	
ν_1 (10^00)	1288.3	1285.4	Fermi doublet
ν_2^2 (02^20)	1338.2	1335.1	
ν_2^2 (02^00)	1388.7	1388.2	Fermi doublet
$\nu_1\nu_2$ (11^10)	1937.0	1932.5	Fermi doublet
ν_2^3 (03^30)	2009.6	2003.2	
ν_2^3 (03^10)	2078.6	2076.9	Fermi doublet
ν_3 (00^01)	2349.2	2349.2	

The accidental near degeneracy, $\nu_1 \approx 2\nu_2$, results in a significant anharmonic coupling between the two modes, ν_1-$2\nu_2$ Fermi resonance.

Computational Chemistry

There is always a trade-off in a calculation between the size of the molecule and the required accuracy. Owing to the theoretical developments and high-speed computers, quantum chemistry can now describe the properties of small molecules with chemical accuracy (2 kcal/mol or 0.1eV) comparable to those of experiment using correlated *ab initio* method but for biological/nano-scaled molecules we have to be content with cruder treatments.

Nano-Bio Simulation

With the emergence of peta-scale computing platforms we are entering a new period of modeling. The computer simulations can be carried out for larger, more complex, and more realistic systems than ever before.

BIO(Chaperones)

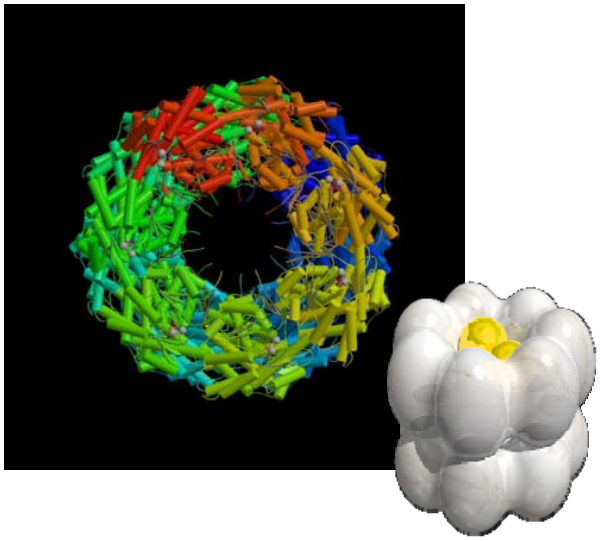

SOFT(Light-Harvesting LC)

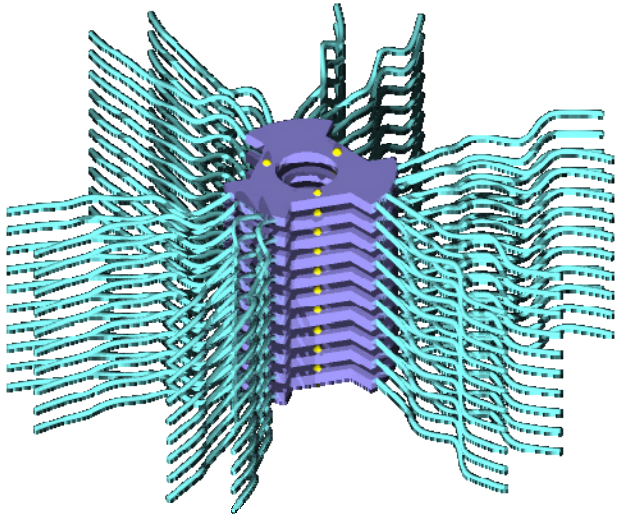

HARD(Mesoporous)

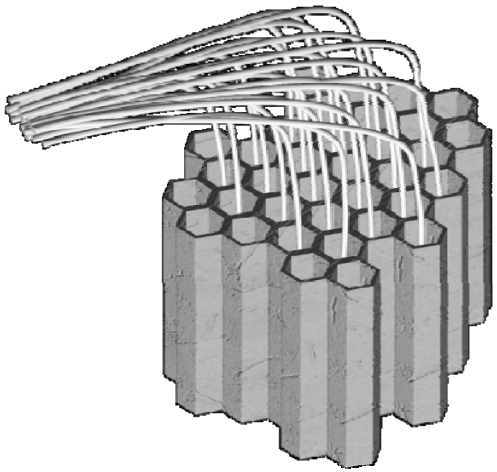

Next Generation Supercomputer Project in Japan

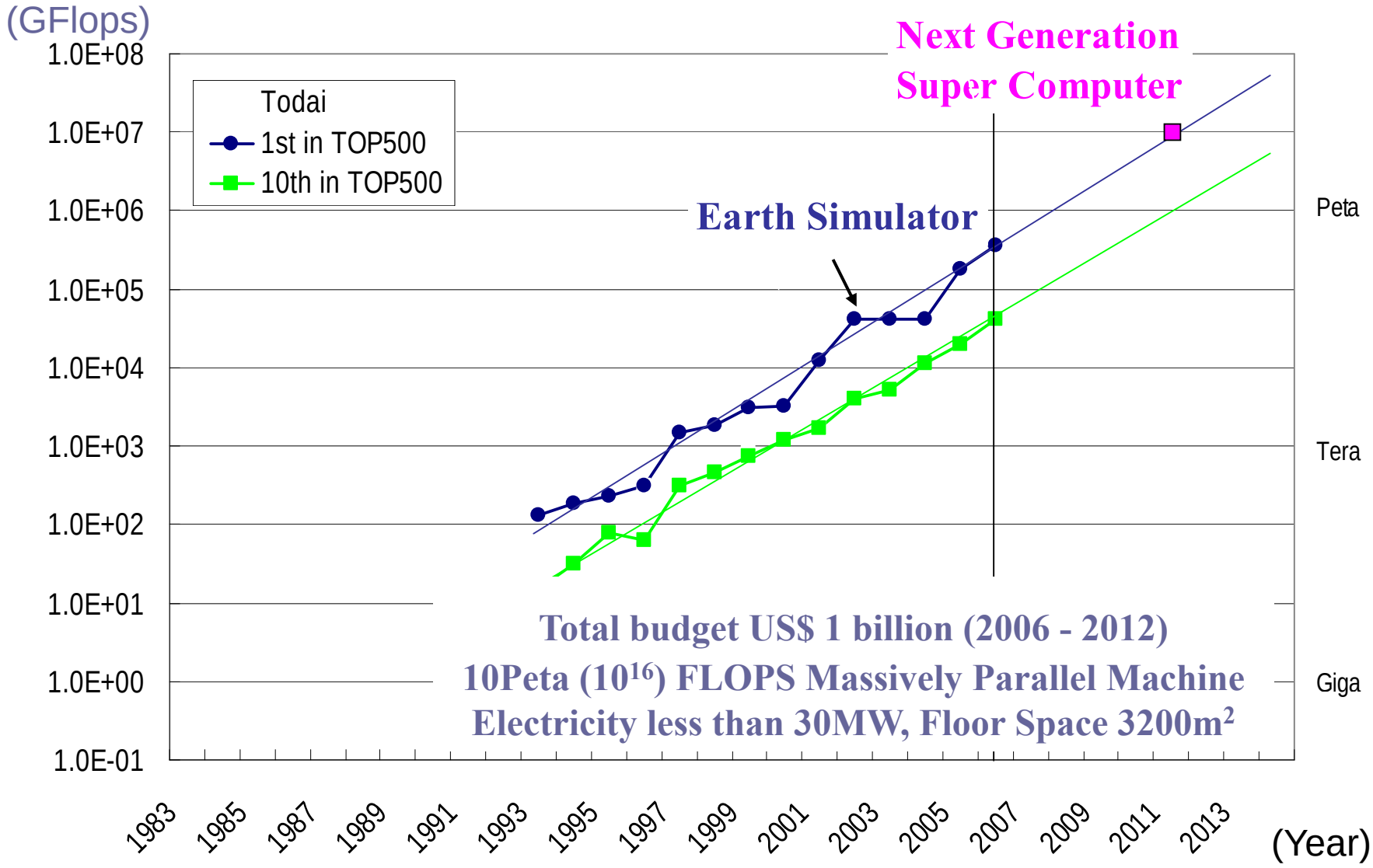

The bane of ab initio calculations

Steep *N* dependence of the computational efforts on the system size, *N*

The dependence is of order N^3 for SCF, Kohn-Sham, and is of order N^6 and higher for correlated methods beyond MP2.

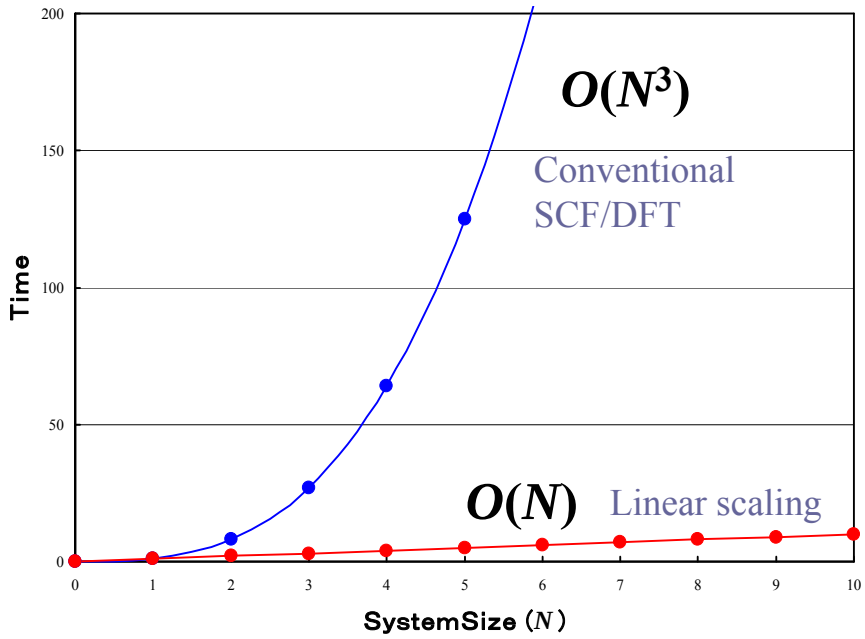

Method/algorithm to reduce *N*-dependence is required

Density Functional Theory (DFT)

DFT may be the only tool that enables us to carry out accurate simulations for larger systems with reasonable computational cost. If practical DFT is developed, which can handle biomolecules and nanomaterials, we can enlarge greatly the scope of computational chemistry.

Topics

- *Fast Evaluation of Coulomb Integrals with Gaussian and Finite Element Coulomb Method*

- *Kohn-Sham Method without SCF Procedure*

- *Accurate Description of van der Waals Interactions*

Gaussian and Finite Element Coulomb (GFC) Approach

Y.Kurashige, T.Nakajima, and K.Hirao,
J.Chem.Phys., **126**, 144106 (2007)

Three time-consuming steps for DFT with GGA

- **Numerical integration of exchange-correlation (*xc*) part**

  can be implemented in linear-scaling fashion using Becke's weighting scheme

- **Coulomb part**

  is very often the most time consuming one, in particular with GGA functionals

- **Diagonalization of Fock matrix**

  scales cubically but insignificant compared to that of the computation of either *xc* or Coulomb for systems with up to several thousands basis functions

Fast Numerical Methods

Much effort has been made to develop efficient methods in evaluation of Coulomb integrals. Integral prescreening technique reduces the scaling from *O(N⁴) to O(N²)*. Furthermore several efficient computational methods have been proposed.

Auxiliary functions

Gaussians Fast Multipole Moment Method (FMM), ~ *O(NlogN)*.

White, Johnson, Gill, Head-Gordon, JCP(1996)

Resolution of the Identity (RI) Approach, *Vahtras, Almlof, Feyerisen, CPL(1993)*

$$J_{pq} = \sum_{A}^{M} (pq|A) \sum_{B}^{M} \left[(A|B)^{-1} \left(\sum_{rs}^{N} D_{rs} (B|rs) \right) \right]$$

4c ERIs are decomposed into 3c and 2c ERIs.

Plane waves Mixed Basis Method, ERI with PW scales as ~ *O(M)*.

Lippert, Hunter, Parrinello, MP(1997), Fusti-Molnar, Pulay, JCP(2002), Kurashige, Nakajima, Hirao, CPL(2006)

$$J_{pq} = J_{pq}^{Gauss} + J_{pq}^{GAU-PW} = J_{pq}^{Gauss} + \sum_{h}^{M} w_h R_p^S(h) R_q^S(h) J^S(h), \quad J^S(k) \frac{4\pi}{k^2} \rho^S(k) \qquad k-space$$

Grid basis Pseudospectral (PS) Method, ~ *O(N²M)*. PS combines analytical basis sets with numerical grid basis functions, *Friesner CPL(1985), Nakajima, Hirao, JCP(2004)*

$$J_{pq} = \sum_{g}^{M} w_g R_p(g) R_q(g) \left(\sum_{rs}^{N} D_{rs} A_{rs}(g) \right), \quad A_{rs}(g) = \int \frac{\chi_r(g')\chi_s(g')}{|g-g'|} dg'$$

Gaussian and Finite Element Coulomb Approach

Coulomb integrals are given with Gaussians and Coulomb potentials

$$J_{pq} = \int dr \chi_p(r) \chi_q(r) v(r)$$

$$v(r) = \int dr' \frac{\rho(r')}{|r'-r|}, \qquad \rho(r') = \sum_{rs} D_{rs} \chi_r(r') \chi_s(r')$$

We expand Coulomb potentials in terms of auxiliary functions, Gaussians and Finite Element Basis as

$$v(r) = \sum_i c_i^{FE} f_i^{FE}(r) + \sum_i c_i^{Gauss} f_i^{Gauss}(r)$$

The atom-centered Gaussian functions represent the spherical core potential near a nucleus, while uniform finite-element functions, a tensor product of one-dimension Lagrange interpolate polynomials, represent the residual, which would be smooth across the board.

Coulomb Integrals

Coulomb integrals can be evaluated by overlap integrals among two Gaussian basis functions and one auxiliary function

$$
\begin{aligned}
J_{pq} &= \int dr \chi_p(r) \chi_q(r) v(r) \\
&= \sum_i c_i^G \int dr \chi_p(r) \chi_q(r) f_i^G(r) + \sum_i c_i^{FE} \int dr \chi_p(r) \chi_q(r) f_i^{FE}(r)
\end{aligned}
$$

No four-center two-electron integrals

Drastically reduces the computational cost

Poisson's Equation

The expansion coefficients $\{c_i\}$ can be obtained by solving Poisson's equation, which is solved algebraically by the Galerkin method

$$-\nabla^2 V(r) = 4\pi\rho(r) \xrightarrow[\text{functions}]{\text{auxiliary}} \begin{bmatrix} \mathrm{O} & & 0 \\ & \mathbf{A} & \\ 0 & & \mathrm{O} \end{bmatrix} \times \begin{bmatrix} \mathrm{M} \\ \mathbf{c} \\ \mathrm{M} \end{bmatrix} = \begin{bmatrix} \mathrm{M} \\ \mathbf{b} \\ \mathrm{M} \end{bmatrix}, \quad \begin{cases} \mathbf{A}_{\mathrm{ij}} = \underbrace{\int \nabla f_i(r) \cdot \nabla f_j(r) dr}_{\text{kinetic integral}} \\ \mathbf{b}_i = \underbrace{\int \rho(r) \cdot f_i(r) dr}_{\text{overlap integral}} \\ V(r)\,; \quad \sum_i \mathbf{c}_i \cdot f_i(r) \end{cases}$$

- The linear equation is solved by using CG method.
- The matrix A is independent of $\rho(r)$ and contains only kinetic-like integrals. It is extremely sparse in the localized auxiliary basis functions.
- Poisson's equation scales as $O(N)$.

Performance

CPU：IBM Power 4 1.0GHz BLYP／SVP

Analytical and FMM results are computed using GAMESS

Table I Equilibrium bond lengths (R_e), harmonic frequencies (ω_e), atomization energies (D_e) and equilibrium total energies (E_{KS}) for diatomic molecules using BLYP/6-31G**

	Analytical integrals				GFC method			
	R_e(Å)	ω_e(cm^{-1})	D_e(kcal/mol)	E_{KS}(hartree)	R_e(Å)	ω_e(cm^{-1})	D_e(kcal/mol)	E_{KS}(hartree)
BeH	1.354	2036	57.1	-15.2422	1.354	2035	57.1	-15.2423
CH	1.146	2725	84.7	-38.4604	1.145	2727	84.8	-38.4607
CN	1.187	2112	189.2	-92.6979	1.187	2111	189.3	-92.6981
CO	1.150	2153	260.6	-113.2907	1.150	2153	260.7	-113.2911
F_2	1.437	994	55.4	-199.4907	1.436	991	55.6	-199.4912
FH	0.936	4016	133.7	-100.4097	0.938	4012	134.0	-100.4103
H_2	0.747	4485	111.1	-1.1679	0.747	4488	111.1	-1.1680
Li_2	2.732	335	20.2	-14.9922	2.734	335	20.2	-14.9923
LiF	1.561	1051	137.8	-107.4008	1.561	1051	137.8	-107.4010
LiH	1.623	1377	57.1	-8.0664	1.622	1376	57.1	-8.0665
N_2	1.118	2388	234.4	-109.5063	1.116	2387	235.2	-109.5076
NH	1.060	3163	87.7	-55.2015	1.059	3164	88.0	-55.2021
NO	1.176	1909	165.3	-129.8753	1.175	1914	166.1	-129.8767
O_2	1.239	1551	138.4	-150.311 6	1.239	1552	138.7	-150.3123
OH	0.992	3617	106.2	-75.7102	0.991	3619	106.3	-75.7105
MAE	-	-	-	-	0.0006	2	0.2	0.0004

Gaussian and FE Coulomb Approach

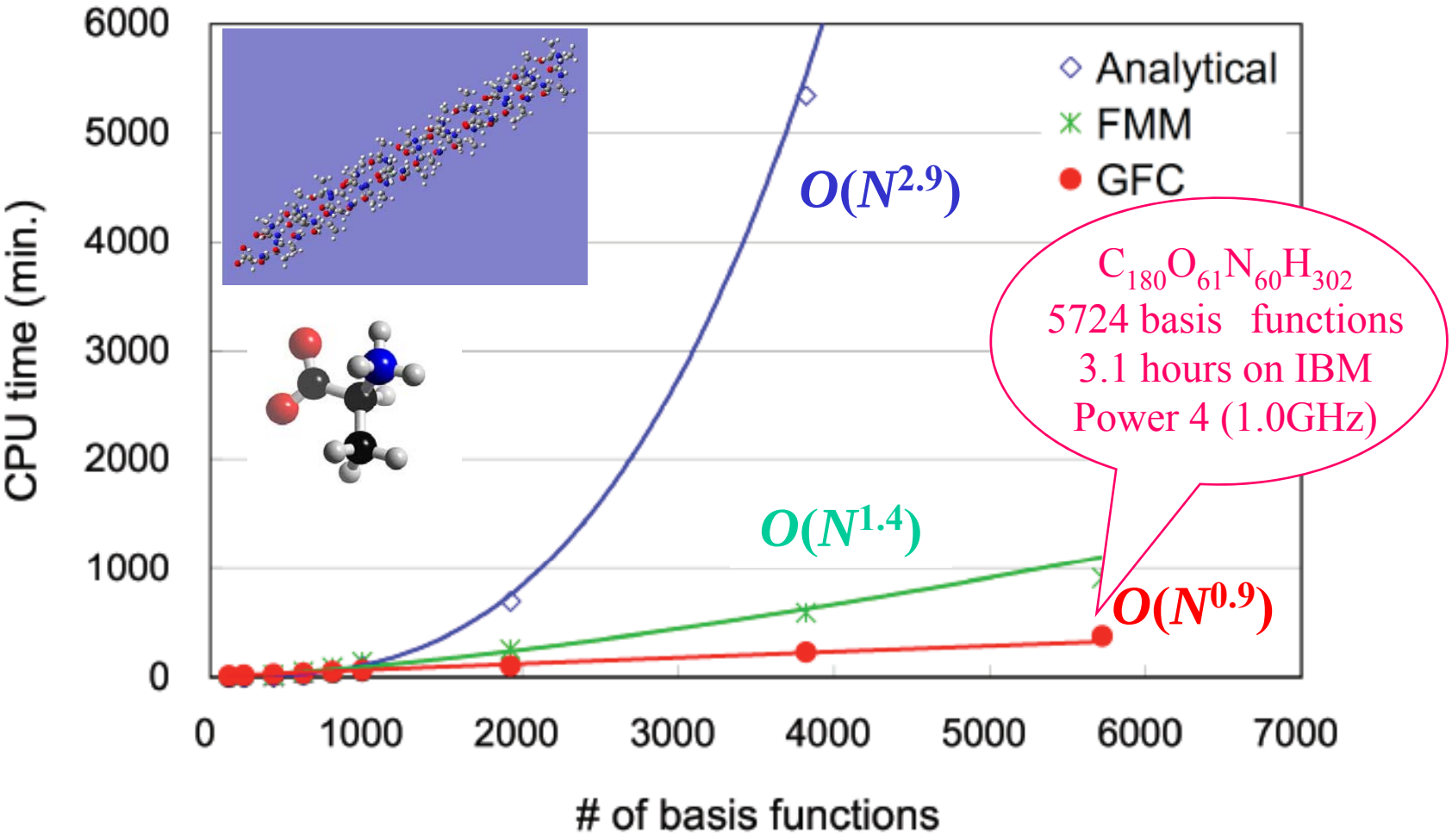

1D Alanine α-helix chain/ SVP

Gaussian and FE Coulomb Approach

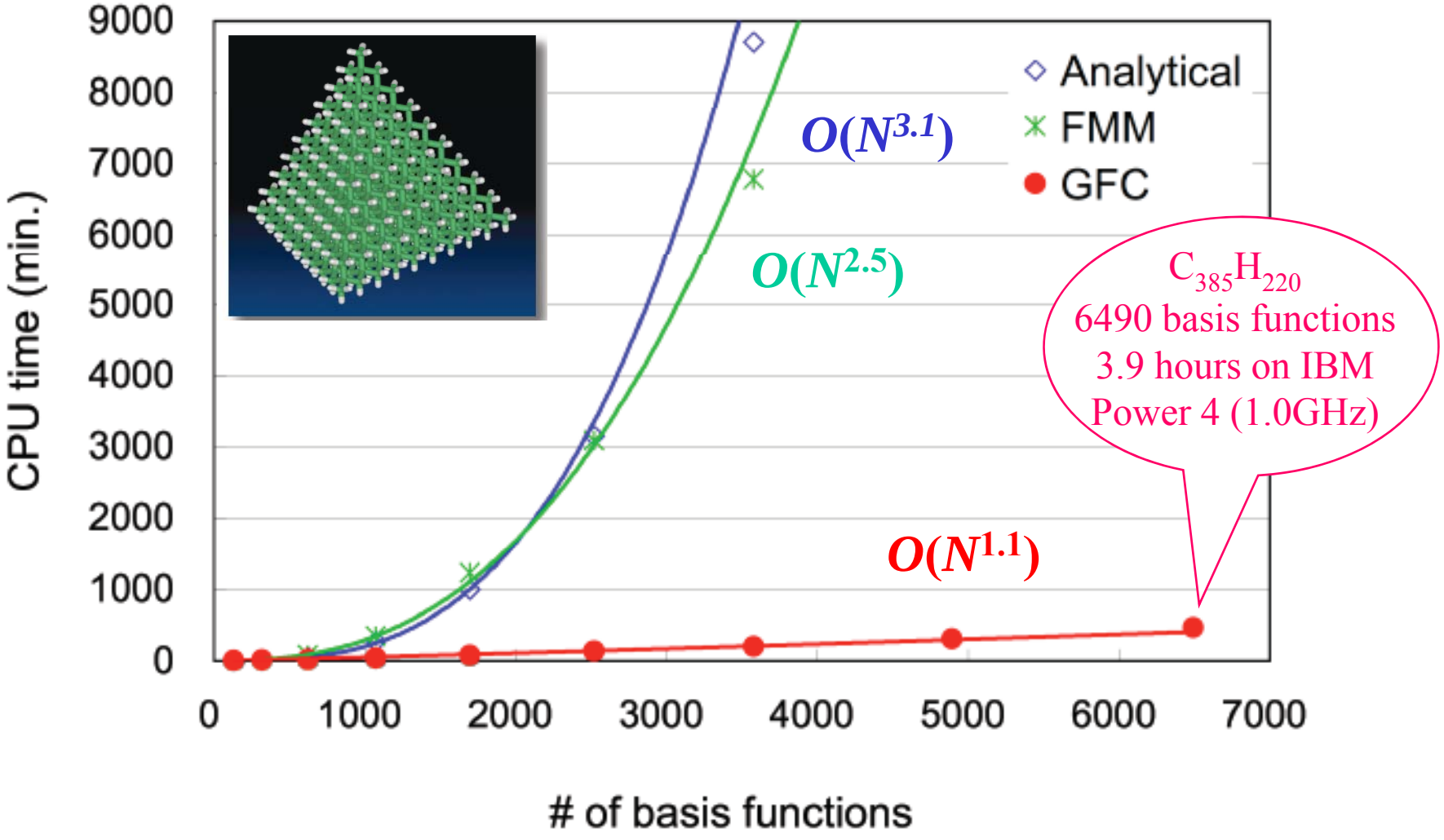

3D diamond/ SVP

Gaussian and FE Coulomb Approach

Gaussian and FE Coulomb approach offers the best performance for evaluating Coulomb integrals without loss of accuracy. The algorithm is found to scale linearly with system size.

Gaussian and FE Coulomb approach makes the molecular quantum calculations affordable for very large systems involving several thousands of basis functions.

Hybrid GGA Functionals

The success of Kohn-Sham DFT was the development of *xc* functionals depending on density gradients in addition to the density itself (GGA).

A further advance is the mixing of a small fraction of exactly computed HF exchange with GGA exchange such as B3LYP, LC-GGA, etc.

Although hybrid GGA improves the accuracy, it also makes the calculation more expensive.

Exchange Integrals

Fast algorithms for Coulomb interaction cannot be employed for HF exchange because its algebraic structure is not compatible with them.

Only the pseudospectral method can be applied to HF exchange but it scales as $O(N^2M)$.

$$J_{pq} = \sum_{g}^{M} w_g \chi_p^*(g)\chi_q(g)\left(\sum_{rs}^{N} D_{rs}A_{rs}(g)\right), \quad K_{pq} = \sum_{g}^{M} w_g \chi_p^*(g)\left[\sum_{r}^{N}\left(\sum_{s}^{N} D_{rs}\chi_s(g)\right)A_{rq}(g)\right]$$

$$A_{pq}(g) = \int \chi_p^*(1)\frac{1}{|r_1 - r_g|}\chi_q(1)dr_1$$

Friesner CPL(1985), Nakajima and Hirao, JCP(2004)

The hybrid GGA is more accurate but less efficient for large systems.

Dual-Level Approach

Nakajima and Hirao, *J.Chem.Phys.*, **124**, 184108 (2006)

To perform hybrid GGA DFT calculations for large systems, we have developed the dual-level approach. The approach is based on the low sensitivity of the density to the choice of the functional and the basis set. The total electron density in the ground state can be well represented in terms of the density evaluated using the low-quality basis set and the low-cost *xc* functional.

The error is remedied by the second-order perturbation theory.

Dual-Level DFT

Solve KS equation
with low-quality basis set & low-level functional
and obtain a total density

⇩

Use a frozen density approximation
and evaluate the total energy
with high-quality basis set & high-level functional

Total Electronic Energy

The reference energy of the KS total electronic energy is given by

$$E_{KS}^{(0)} = 2\sum_{pq} D_{pq} h_{pq} + 2\sum_{pq}\sum_{PQ} D_{pq} D_{PQ}^{L} \left(pq|PQ\right) - t_{EX} \sum_{pq}\sum_{PQ} D_{pq} D_{PQ}^{L} \left(pQ|Pq\right) + t_{XC} E_{XC}$$

Since no rotations between occupied and virtual orbitals are allowed, Brillouin theorem is not satisfied. The correction to the KS energy is evaluated perturbatively by

$$E_{KS}^{(1)} = 2\sum_{i}^{occ}\sum_{a}^{vir} \frac{\left|F_{ia}\right|^2}{\varepsilon_i - \varepsilon_a}$$

The KS total electronic energy is given by

$$E_{KS} = E_{KS}^{(0)} + E_{KS}^{(1)}$$

Timing of Dual-Level DFT

Timing of dual-level DFT

	# of basis functions	Lower level (h:m:s)	Higher level (h:m:s)	Total cpu (h:m:s)	Total Energy (au)
B3LYP	1944	-------	925:47:11	925:47:11	-3794.9350
B3LYP:LDA	882	2:52:08	12:24:07	15:16:15	-3794.9509

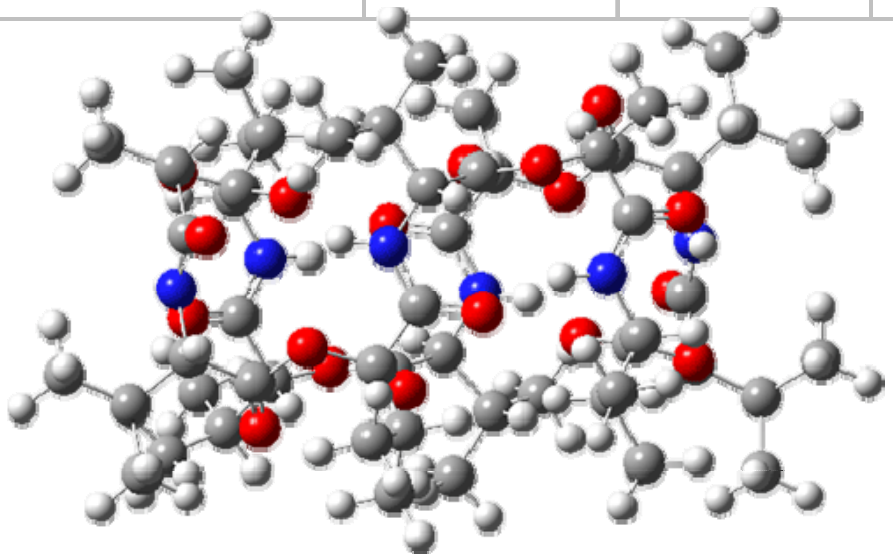

60.6 times faster

(38 days → 15 hours)

Valinomycin
($C_{54}H_{90}N_6O_{18}$)

Calculated interaction energies (kcal/mol)

	B3LYP/ 6-31G**	B3LYP/ 6-31G	LDA/ 6-31G	B3LYP: LDA
Cytosine–guanine pair				
Cytosine	-394.7170	-394.5888	-391.5696	-394.7204
Guanine	-542.2618	-542.0766	-537.9595	-542.2675
Cytosine–guanine	-937.0284	-936.7218	-929.6077	-937.0374
Interaction Energy	31.1	35.4	49.3	31.1
Adenine–thymine pair				
Adenine	-467.0603	-466.8967	-463.2617	-467.0635
Thymine	-453.8940	-453.7501	-450.3102	-453.8996
Adenine–thymine	-920.9806	-920.6786	-913.6204	-920.9894
Interaction Energy	16.5	19.9	30.4	16.5

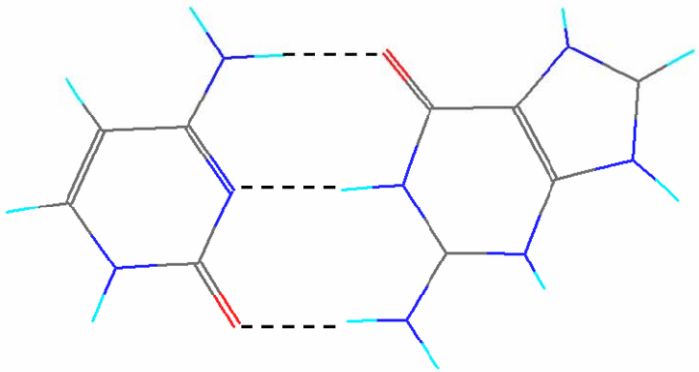

Cytosine-Guanine

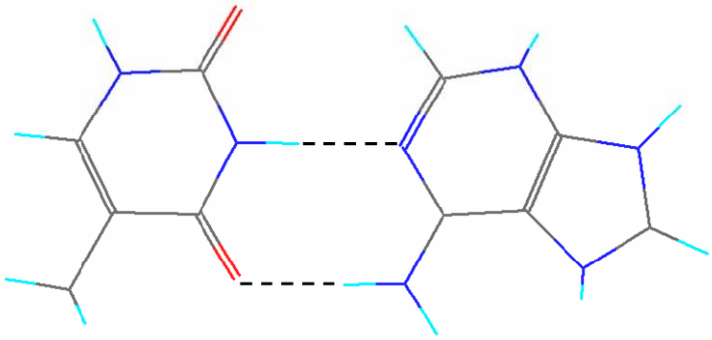

Thymine-Adenine

東京大学
THE UNIVERSITY OF TOKYO

Conclusions

The dual-level DFT approach works quite well and the large reduction of the computer resources can be achieved at an affordable loss of accuracy since the SCF procedure is avoided. Hybrid functionals can now be applied to bio- and/or nano-scaled molecules.

Hybrid GGA functional with correct long-range electron-electron interactions

J.Chem.Phys., submitted.
J. Chem.Phys., **126**, 154105 (2007)
J.Chem.Phys., **120**, 8425 (2004)
J. Chem.Phys., **115,** 3540 (2001)

Conventional GGA has problems

1. Barrier heights in chemical reactions underestimated.
2. Van der Waals interactions repulsive
3. Excitations using time-dependent DFT for Rydberg and CT states underestimated
4. Band gaps of insulators too small
5. Optical response function too large
6. And, and, and,…

Since

1. *xc* potential decays as $\exp(-\alpha r)$ rather than $-1/r$
2. self-exchange & self-Hartree potentials do not cancel

It's possible to improve the asymptotic behavior !

The failure arises from the wrong long range behavior due to the local character of the approximate *xc* functionals.

By splitting the Coulomb interaction into short-range and long-range components, we proposed a new hybrid functional with correct long-range electron-electron interactions.

P.Gill (1996), A.Savin (1996)

The key is the partitioning of $1/r_{12}$ for the exchange contribution

An Ewald partitioning

$$\frac{1}{r_{12}} = \frac{1-erf(\mu r_{12})}{r_{12}} + \frac{erf(\mu r_{12})}{r_{12}}$$

$\Uparrow$ $\Uparrow$

GGA exchange *HF exchange*

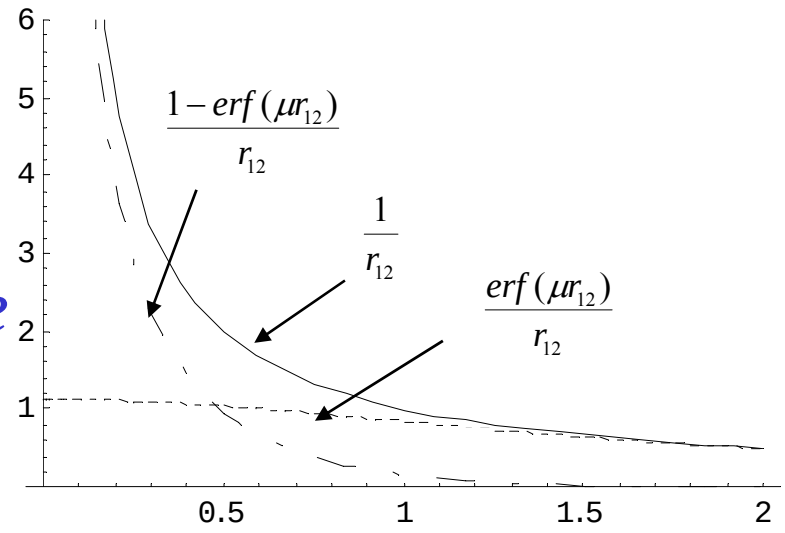

μ *is a parameter controlling the separation* $(\mu = 0.47)$

Andreas Savin (1996)

Exchange functional with correct long-range electron-electron interactions

$$E_x = E_x^{short} + E_x^{long}$$

Long-range: Hartree-Fock exchange

$$E_x^{long} = -\sum_i \sum_j \iint \varphi_i(r_1)\varphi_j(r_1)\frac{erf(\mu r_{12})}{r_{12}}\varphi_j(r_2)\varphi_i(r_2)dr_1 dr_2$$

Short-range: GGA exchange functional

$$E_x^{short} = -\frac{1}{2}\sum_\sigma \int \rho_\sigma^{4/3} K_\sigma \left[1 - \frac{8}{3}a_\sigma \left\{\sqrt{\pi}\, erf\left(\frac{1}{2a_\sigma}\right) + 2a_\sigma(b_\sigma - c_\sigma)\right\}\right]dr$$

$$a_\sigma = \frac{\mu K_\sigma^{1/2}}{6\sqrt{\pi}\,\rho_\sigma^{1/3}}, \quad b_\sigma = \exp\left(-\frac{1}{4a_\sigma^2}\right) - 1, \quad c_\sigma = 1a_\sigma^2 b_\sigma + 1$$

Hybrid exchange functionals

B3LYP

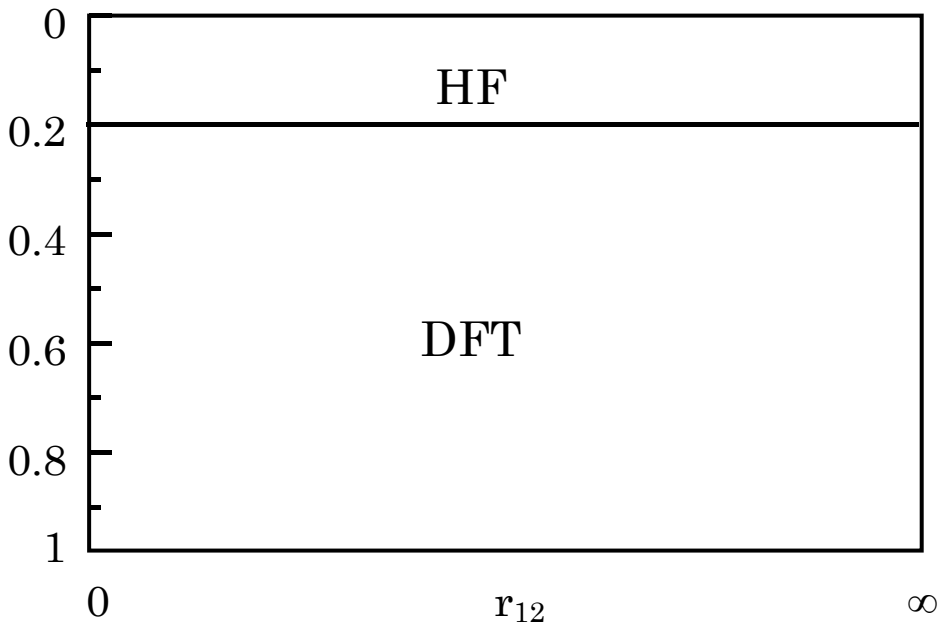

$$E_x^{B3} = 0.2E_x^{HF} + 0.8E_x^{Slater} + 0.72E_x^{B88}$$

Behaves as -0.2r^{-1}

LC - GGA

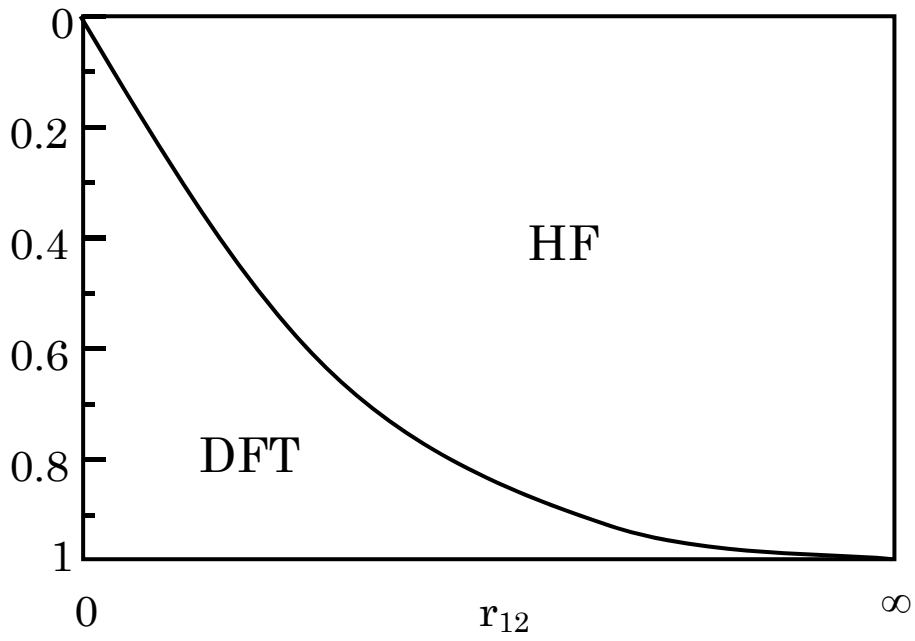

$$\frac{1}{r_{12}} = \frac{1 - erf(\mu r_{12})}{r_{12}} + \frac{erf(\mu r_{12})}{r_{12}}$$

Behaves as -r^{-1} at long-range

Response Properties

Hyperpolarizabilities

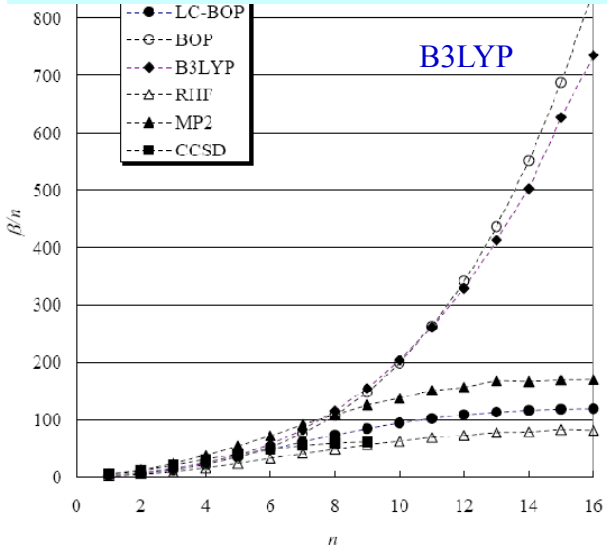

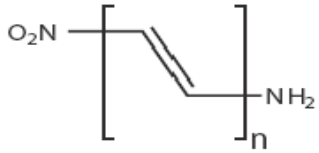

Charge Transfer States

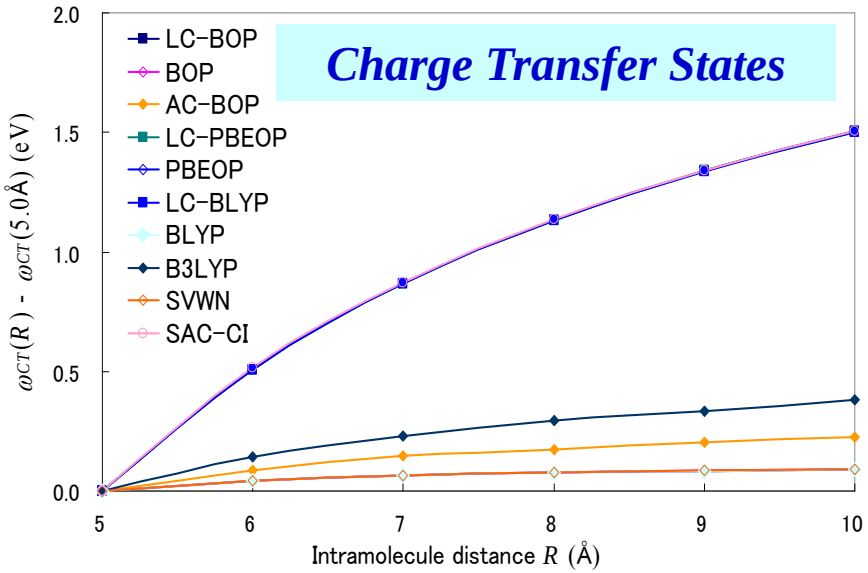

Excitation Energies, MAE (eV)

27 valence excitations (N_2, CO, H_2CO, C_2H_4, C_6H_6)

BLYP	0.36
B3LYP	0.37
LC-BLYP	0.32
SAC-CI	0.37

41 Rydberg excitations (N_2, CO, H_2CO, C_2H_4, C_6H_6)

BLYP	1.54
B3LYP	0.89
LC-BLYP	0.41
SAC-CI	0.19

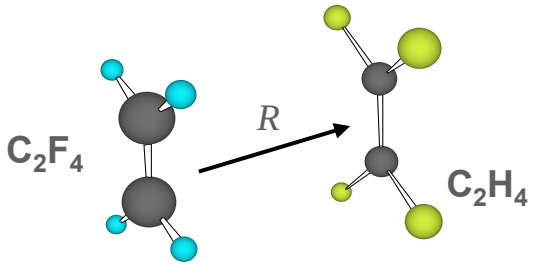

ΔE_{CT}(eV)

BLYP	5.40
B3LYP	7.49
LC-BLYP	12.49
Exptl.	12.5

Rydberg Excitations of Benzene in eV

State	BLYP	B3LYP	LC-BLYP	SAC-CI	Exp.
Valence excitations					
$^1B_{2u}$ $\pi \rightarrow \pi^*$	5.15	5.34	5.38	5.16	4.90
$^1B_{1u}$ $\pi \rightarrow \pi^*$	5.85	6.00	6.20	6.37	6.20
$^1E_{1u}$ $\pi \rightarrow \pi^*$	6.77	6.96	6.97	7.65	6.94
Rydberg excitations					
$^1E_{1g}$ $\pi \rightarrow 3s$	5.53	5.94	6.60	6.55	6.33
$^1A_{2u}$ $\pi \rightarrow 3p\sigma$	6.01	6.42	7.10	7.12	6.93
$^1E_{2u}$ $\pi \rightarrow 3p\sigma$	6.00	6.44	7.25	7.19	6.95
$^1E_{1u}$ $\pi \rightarrow 3p\pi$	6.28	6.67	7.43	7.11	7.41
$^1B_{2g}$ $\pi \rightarrow 3d\sigma$	6.48	6.96	7.89	7.75	7.46
$^1E_{1g}$ $\pi \rightarrow 3d\delta$	6.49	6.97	7.90	7.61	7.54
$^1E_{2g}$ $\pi \rightarrow 3p\pi$	6.73	7.19	8.07	7.94	7.81
Mean absolute deviations					
Valence excitations	**0.29**	**0.26**	**0.24**	**0.23**	**-**
Rydberg excitations	**1.00**	**0.55**	**0.28**	**0.20**	**-**

Free-Base Porphyrin

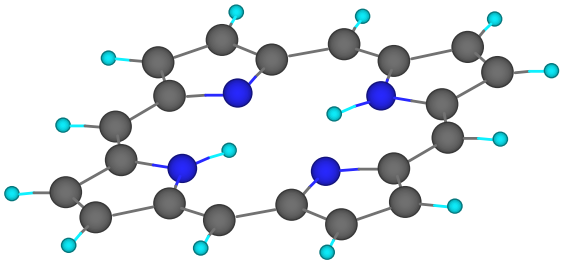

Excitation energy in eV (Oscillator strength)

State	BLYP	B3LYP	LC-BLYP	MRMP	SAC-CI	Exptl
$1\,B_{1u}$	2.16 (0.0010)	2.28 (0.0001)	1.96 (0.005)	1.63 (0.0026)	1.75 (0.0001)	1.98-2.02 (0.02)
$1\,B_{2u}$	2.30 (0.0005)	2.44 (0.0000)	2.28 (0.002)	2.55 (0.0143)	2.23 (0.0006)	2.38-2.42 (0.07)
$2\,B_{1u}$	2.99 (0.11)	3.34 (0.62)	3.59 (2.85)	3.10 (1.61)	3.56 (1.03)	3.13-3.33 (1.15)
$2\,B_{2u}$	3.03 (0.03)	3.51 (0.92)	3.71 (3.63)	3.25 (1.53)	3.75 (1.73)	

Charge Transfer (CT) Excitations

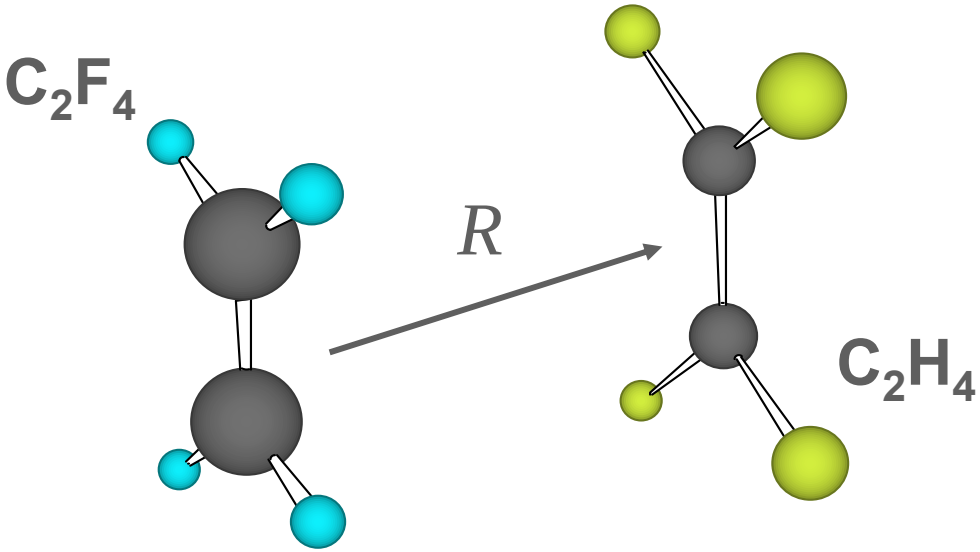

Charge Transfer
from HOMO of C_2F_4
to LUMO of C_2H_4

$$\Delta E_{CT}(R) \cong IP_{tfe} - EA_e - 1/R$$

$$\Delta E_{CT}(R) - \Delta E_{CT}(R_0) \cong -\frac{1}{R} + \frac{1}{R_0}$$

the long-range behavior

$$\Delta E_{CT}(\infty) = IP_{tfe} - EA_e$$

at $R = \infty$

Long-range CT excited states of C_2H_4-C_2F_4

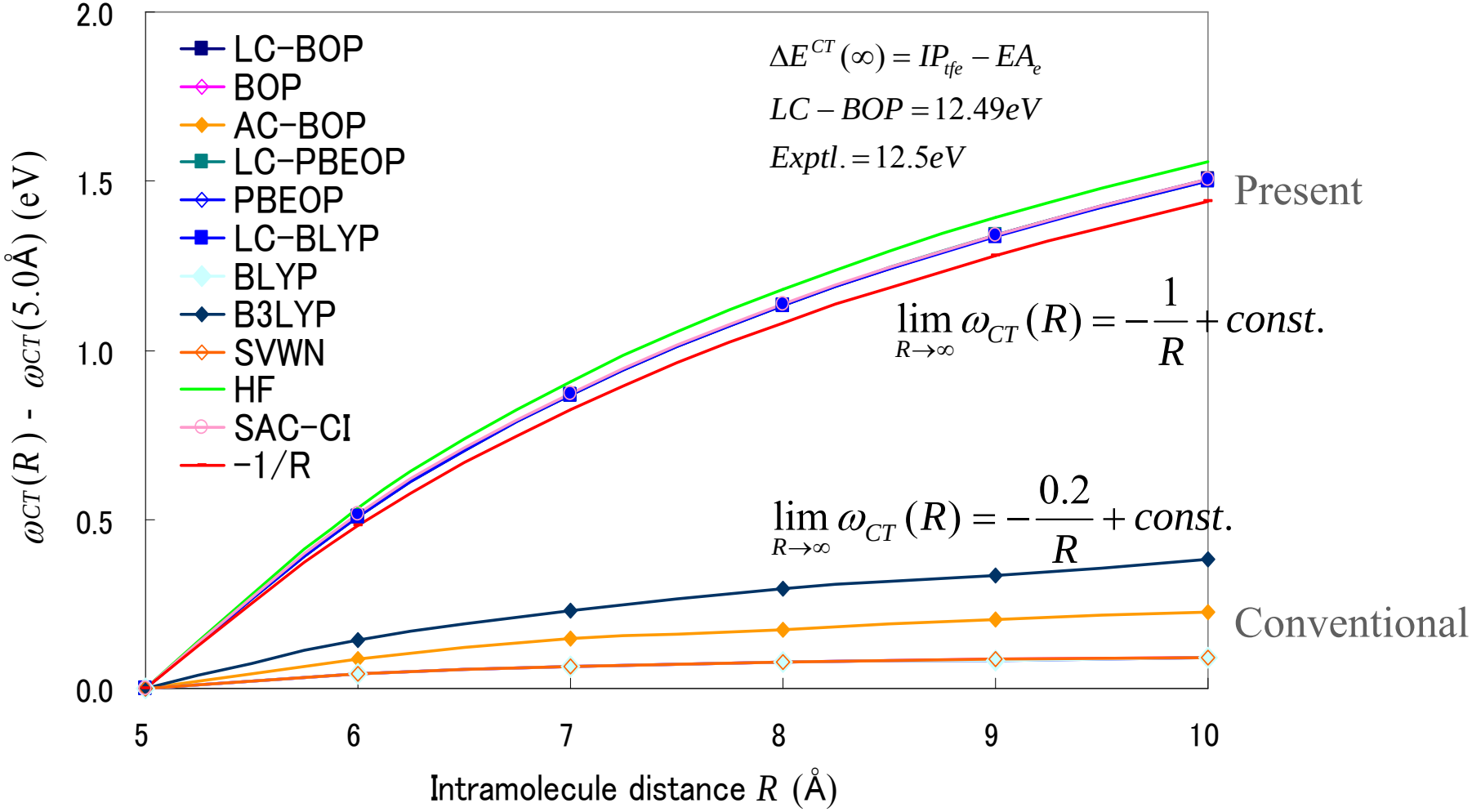

Comparison of the long-range behavior of the lowest CT state of the ethylene-tetrafluoroethylene dimer along the internuclear distance coordinate.

Optimized CT Excited State Geometry
4-cyano-(4'-methylthio)diphenylacetylene

J. Chem.Phys. **124**, 144106 (2006)

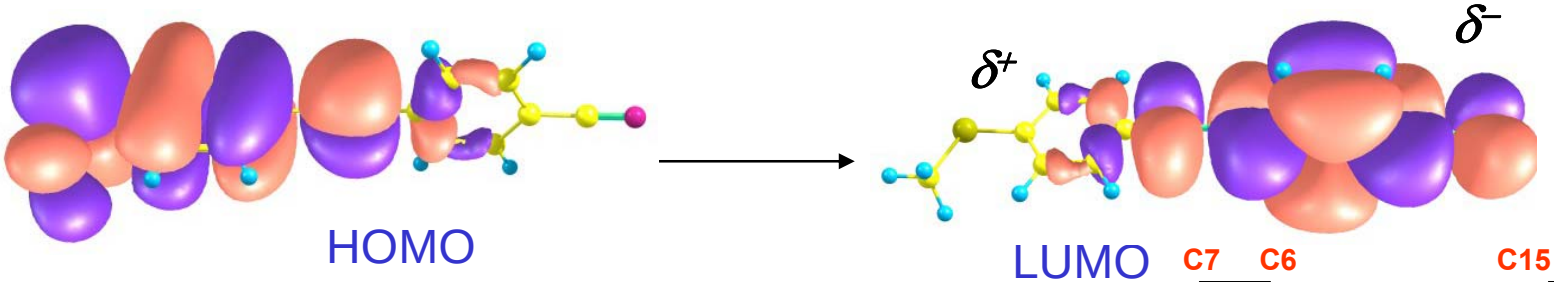

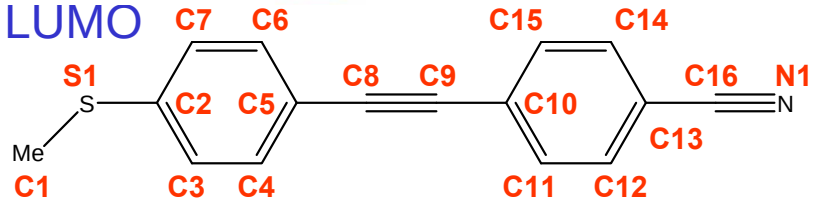

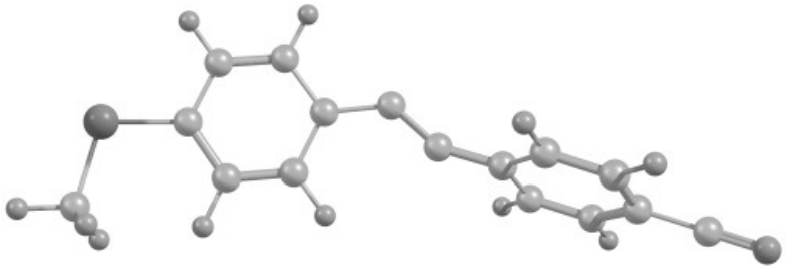

Parameters	BOP	B3LYP	*LC-BOP*
C1-S1	1.83	1.81	1.80
S1-C2	1.77	1.74	1.75
C1-S1-C2	106	105	104
C5-C8	1.44	1.42	1.41
C8-C9	1.27	1.28	1.32
C9-C10	1.39	1.38	1.38
C5-C8-C9	137	136	130
C8-C9-C10	168	168	154
C13-C16	1.41	1.41	1.43
C16-N1	1.19	1.17	1.16

Adiabatic excitation energy (eV)	
BOP	2.37
B3LYP	3.07
LC-BOP	4.02
CASPT2	4.59

Barrier heights (kcal/mol) of chemical reactions

	BOP	B3LYP	LC-BOP	Exp.
$C_2H_6+H \rightarrow C_2H_5+H_2$	2.8	4.9	6.8	7.3
$NH_3+H \rightarrow NH_2+H_2$	4.7	7.5	12.3	11.4
$H_2O+H \rightarrow OH+H_2$	10.9	12.8	18.0	18.5
$H_2O+OH \rightarrow OH+H_2O$	-3.8	3.8	5.9	8.6
$CH_3F+H \rightarrow CH_2F+H_2$	3.4	5.9	9.5	9.0
$CH_3F+H \rightarrow CH_3+HF$	16.8	21.0	24.9	30.1
$CH_3Br+H \rightarrow CH_3+HBr$	0.5	1.9	3.8	5.8
$CH_3Cl+Cl^- \rightarrow Cl^-+CH_3Cl$	-3.8	-2.1	3.8	2.9
$CH_3Br+Br^- \rightarrow Br^-+CH_3Br$	-5.5	-3.9	2.6	1.7
1,2,3,4-$C_2N_4H_2 \rightarrow N_2+2HCN$	27.3	39.7	50.5	51.8
$CH_3Cl+H \rightarrow CH_3+HCl$	3.4	5.2	8.0	10.4
$CH_3Cl+H \rightarrow CH_2Cl+H_2$	3.5	5.9	7.5	11.1
….				
MAE (more than 100 reactions)	**8.7**	**5.6**	**2.6**	

J.Chem.Phys, **126**, 15 4105 (2007)

Hyperpolarizability

α,ω-nitro aminopolyene ($NH_3(CH{=}CH)_nNO_2$)

J.Chem.Phys, **122**, 234111 (2005)

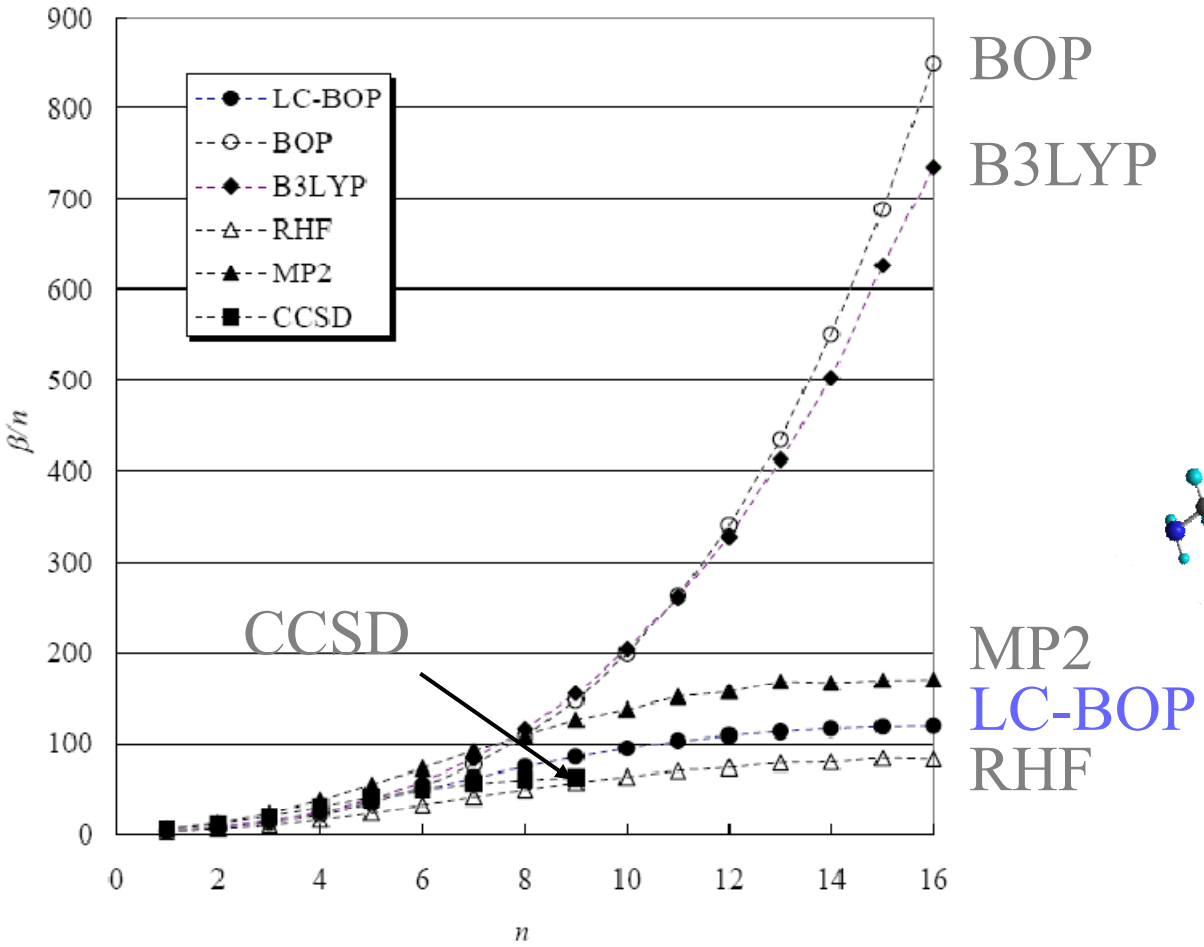

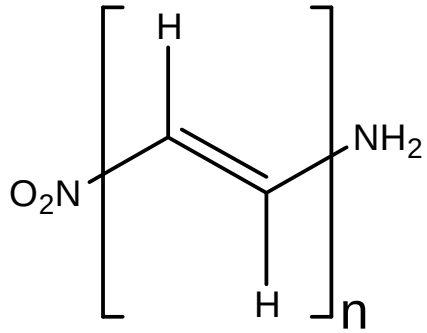

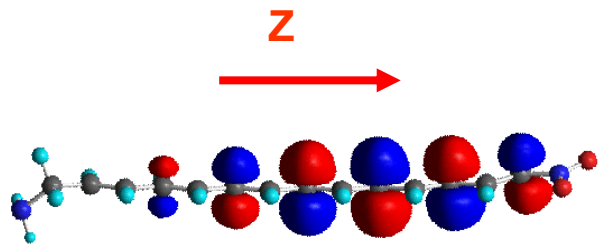

Conclusions

Hybrid functionals can be improved through the introduction of an Ewald partitioning of $1/r_{12}$.

Hybrid GGA functional with correct long-range electron-electron interactions has good energetics, good Rydberg behavior and good CT predictions.

Accurate Description of van der Waals Interactions

Takeshi Sato

J.Chem.Phys., in press.
J. Chem.Phys., **123**, 104307 (2005)
Mol.Phys., **103**, 1151 (2005)
J. Chem.Phys., **117**, 6010 (2002)

Van der Waals interactions

Van der Waals (dispersion) interactions play an important role in many chemical systems. They control the structure of DNA and proteins, the packing of crystals, the formation of aggregates, host-guest systems, the orientation of molecules on surfaces or in molecular films, etc.

Unfortunately almost all GGA DFTs are unable to describe dispersive interactions.

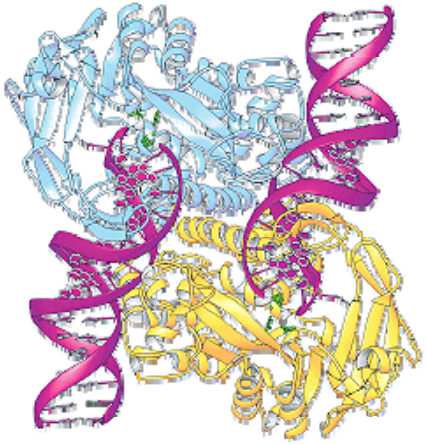

Biomolecules

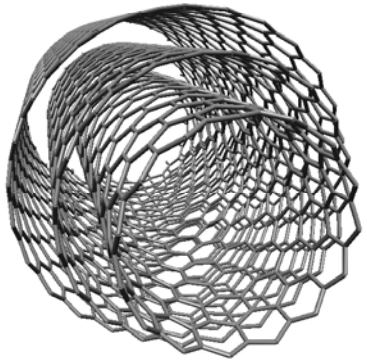

Nanotubes

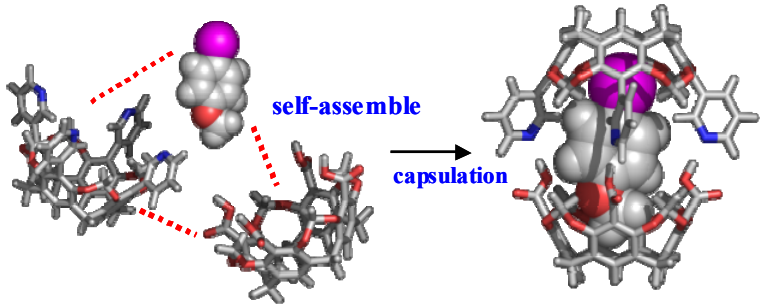

Host-Guest systems

Potential Energy Curves of Ne-Ne

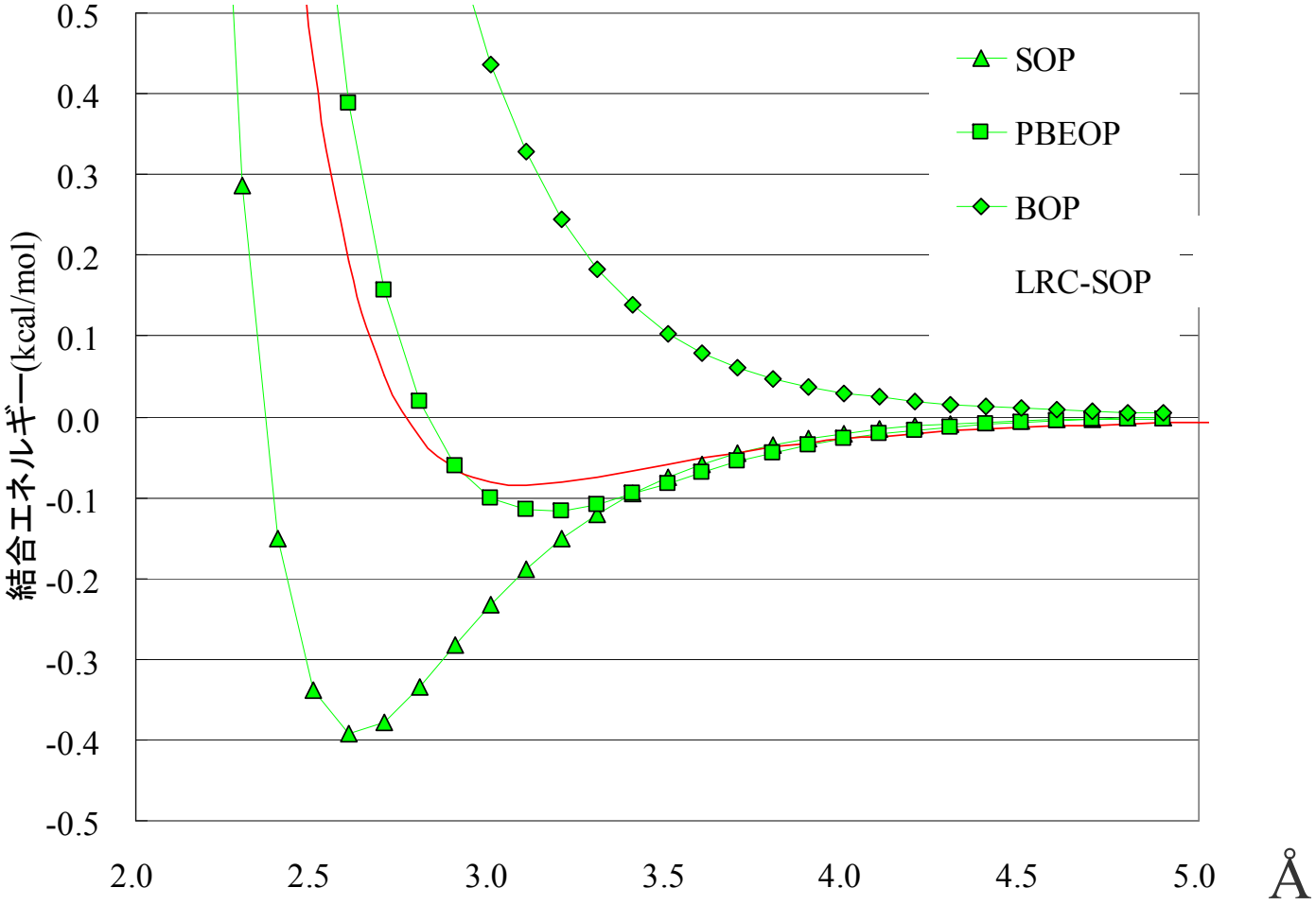

A strong functional dependency appeared in the pure DFT potential

Van der Waals interactions

$$\Delta E^{vdW} = E \text{ (Pauli repulsion) - } E \text{ (Dispersion attraction)}$$

LDA predicts the binding character of vdW interactions. However, LDA severely overestimates the binding energy and yields a too short vdW bond. The GGA predicts repulsive vdW interactions. Thus, none of the functionals account successfully for vdW interactions.

MP2 significantly overestimates the binding energies and MP2 results have strong basis set dependence.
Only CCSD(T) with a large basis set gives the accurate estimation.

Potential Energy Curves of Ne-Ne

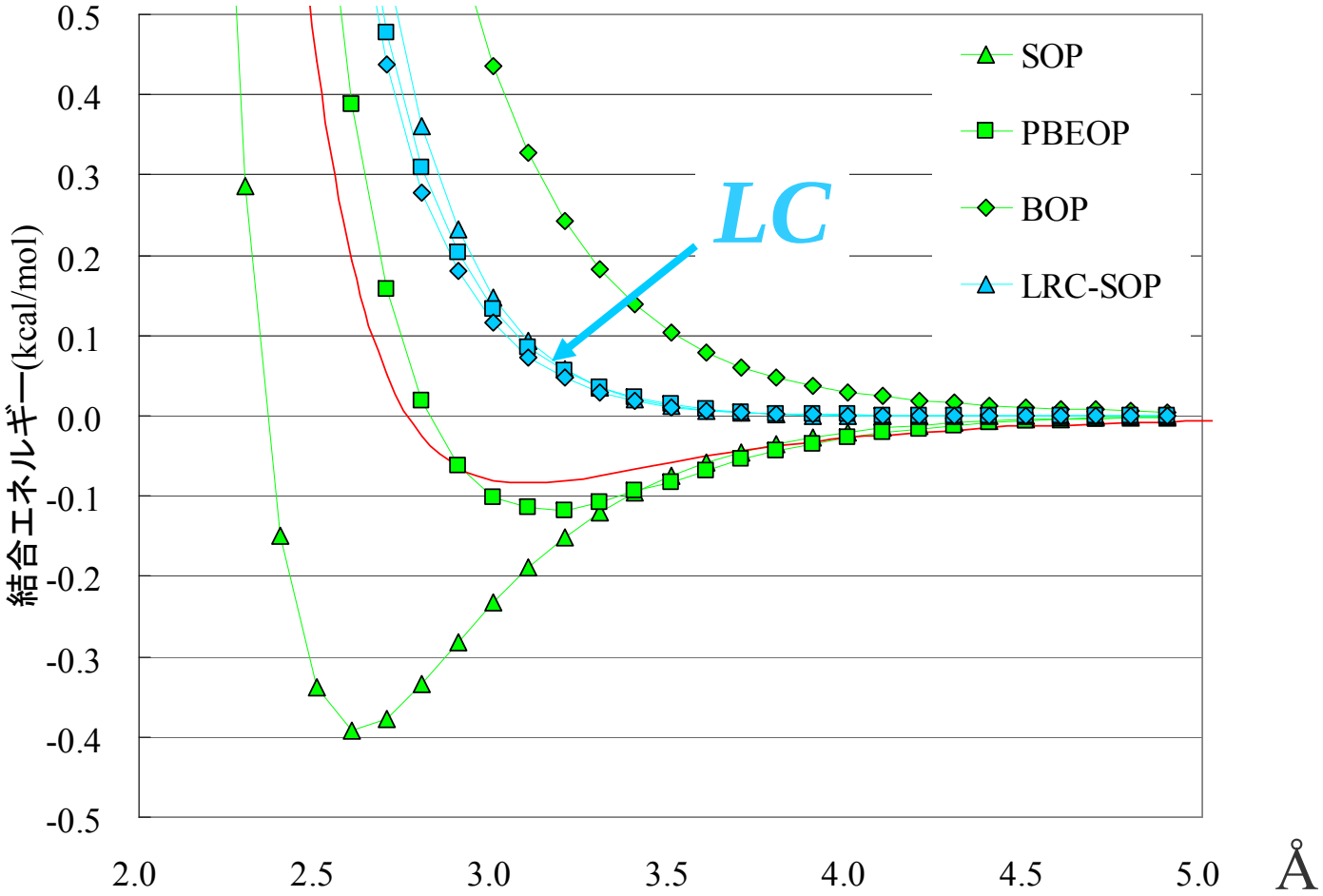

Applying the LC scheme to the exchange functionals leads to similar repulsive potentials

Dispersion Attraction

Van der Waals functional (Andersson et al, PRL 1996)

$$E^{dispersion} = -\frac{6}{4(4\pi)^{3/2}} \int_{V_1} d^3\mathbf{r}_1 \int_{V_2} d^3\mathbf{r}_2 \frac{\sqrt{\rho(\mathbf{r}_1)\rho(\mathbf{r}_2)}}{\sqrt{\rho(\mathbf{r}_1)} + \sqrt{\rho(\mathbf{r}_2)}} \frac{1}{|\mathbf{r}_1 - \mathbf{r}_2|^6}$$

The functional provides an accurate dispersion energy between well-separated electron distributions.

multiplied by a damping factor

$$f_{damp} = \exp\left[-\left(\frac{\alpha_{AB}}{r_{12}}\right)^6\right] \qquad (\alpha_{AB} = C_1 R_{AB} + C_2)$$

R_{AB} : Clementi's atomic radii (1963)

Potential Energy Curves of Rare-gas Dimers

Basis set: aug-cc-pVTZ, BSSE-corrected

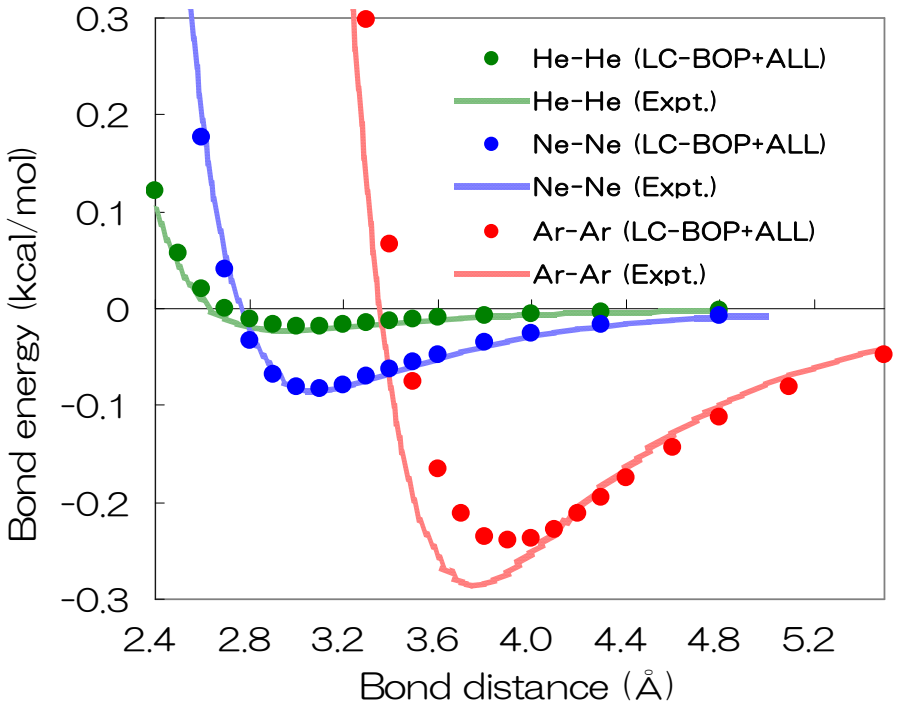

Homo-nuclear

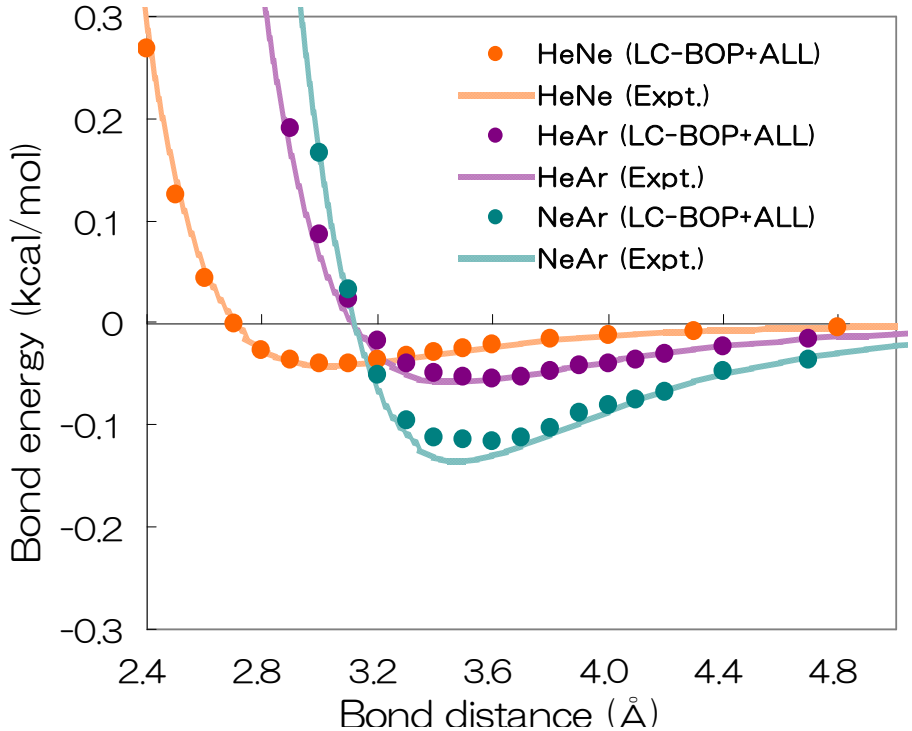

Hetero-nuclear

Contour plot of the PES of FCl--He

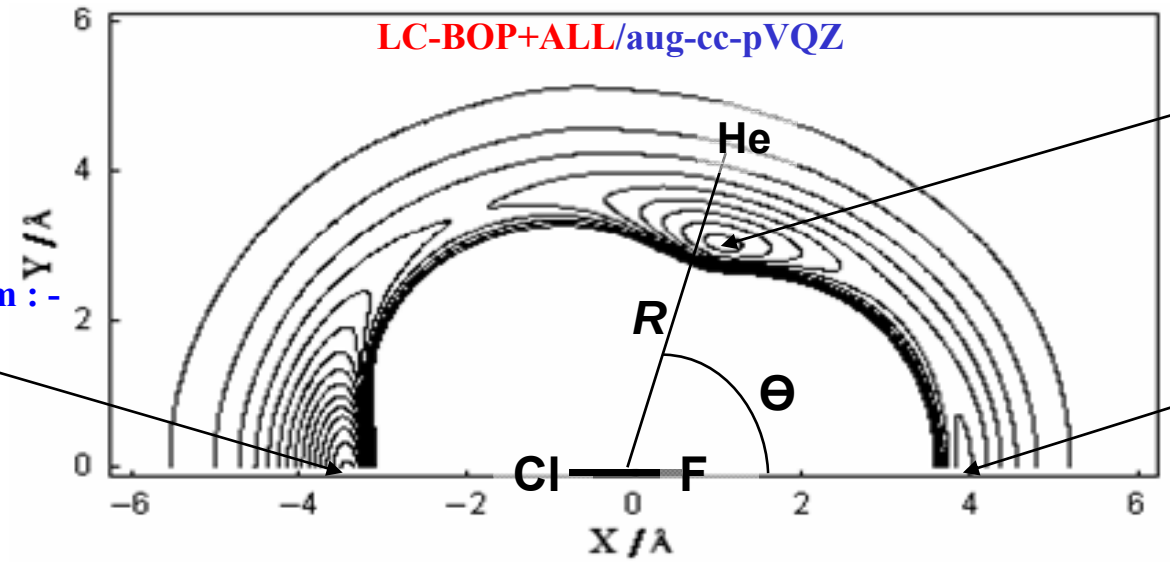

T-shaped minimum:

46.53 cm^{-1}

(Re=3.19 Å,θe=70.0°)

Collinear minimum : -76.43 cm^{-1}

(Re = 3.41 Å)

Antilinear minimum:

30.04 cm^{-1}

(Re=3.91 Å)

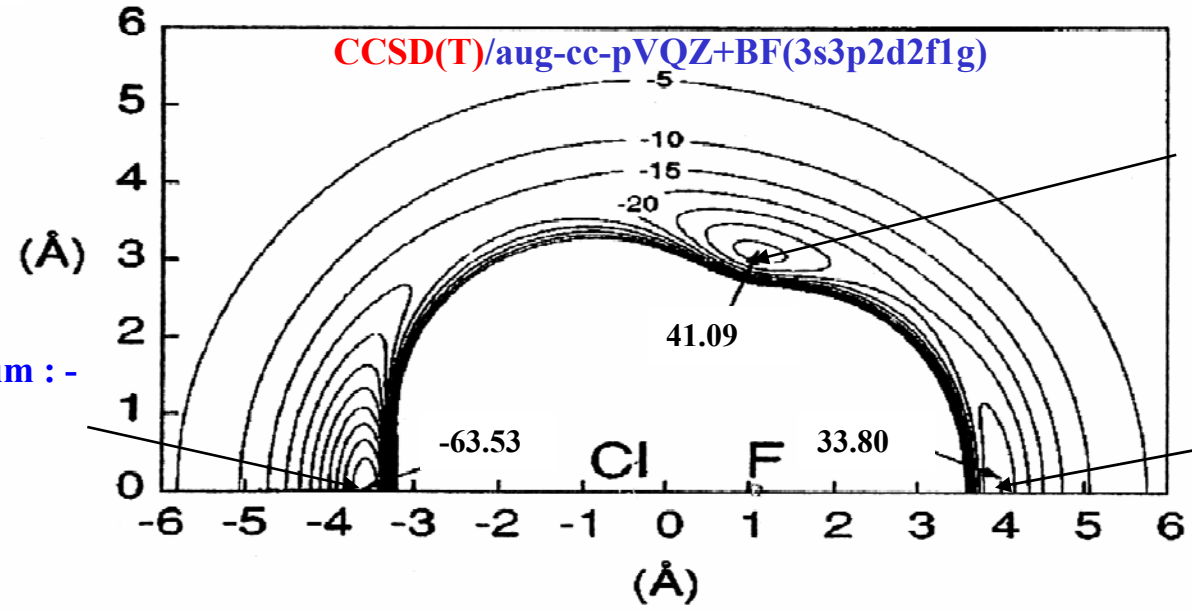

T-shaped minimum:

41.09 cm^{-1}

(Re=3.23 Å,θe=70.1°)

Collinear minimum : -63.53 cm^{-1}

(Re = 3.54 Å)

Antilinear minimum:

33.80 cm^{-1}

(Re=3.95 Å)

Mol.Phys.(Handy special issue), **103**, 1151 (2005)

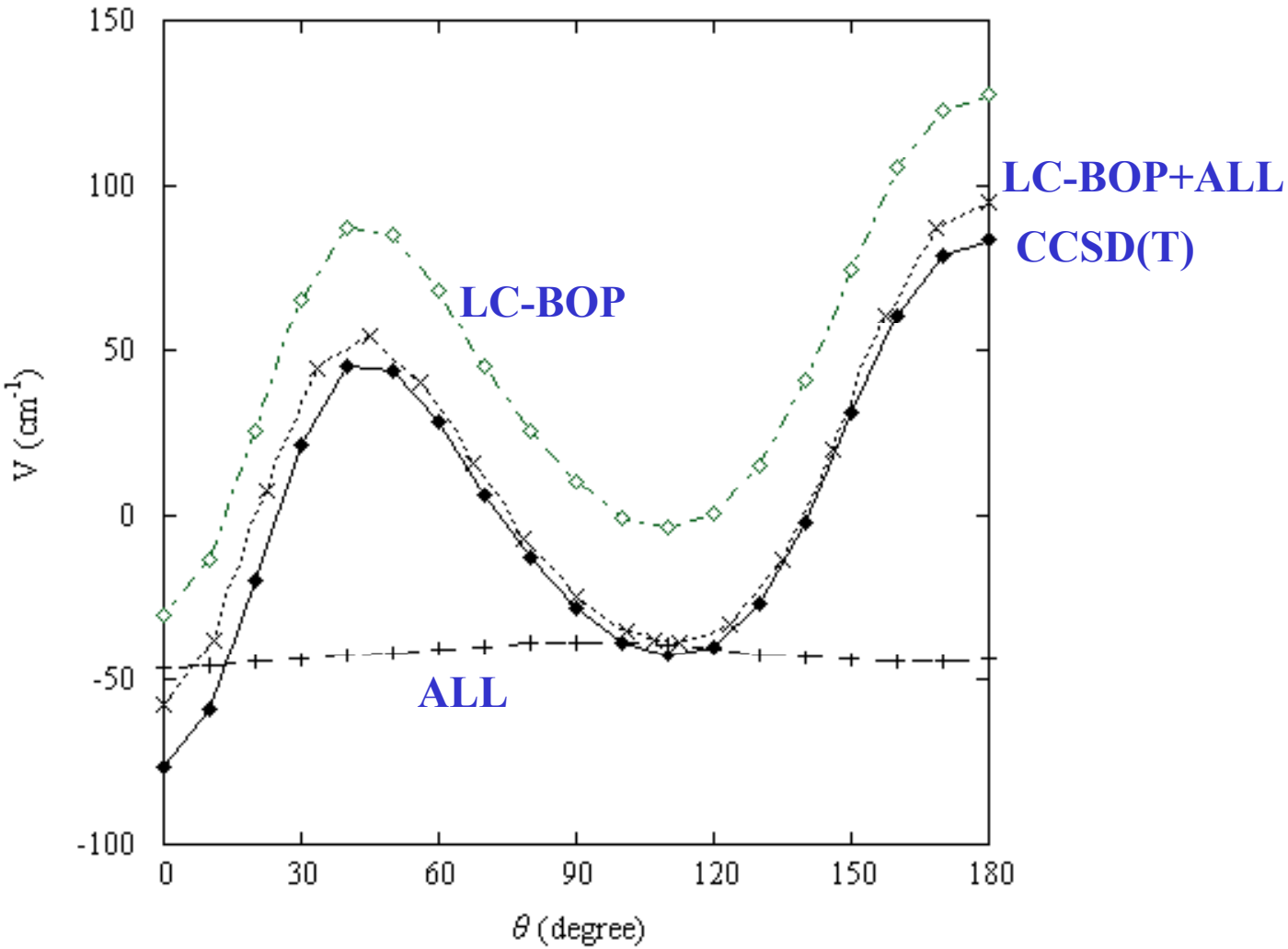

Component energies of FClHe in cm^{-1}.
Intermonomer distance (R) is fixed at 3.4 Å.

LC plays a major role in the determination of vdW complex structure.

Benzene Dimer

J.Chem.Phys., **123**, 104307 (2005)

All previous GGA-DFT predicted repulsive vdW interactions

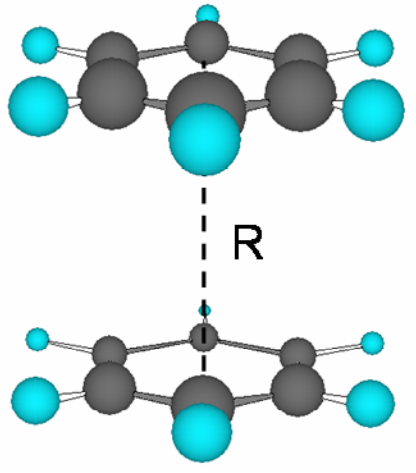

Parallel

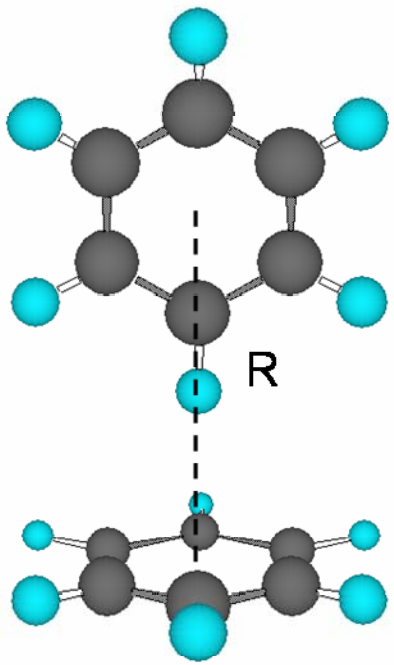

T-Shape

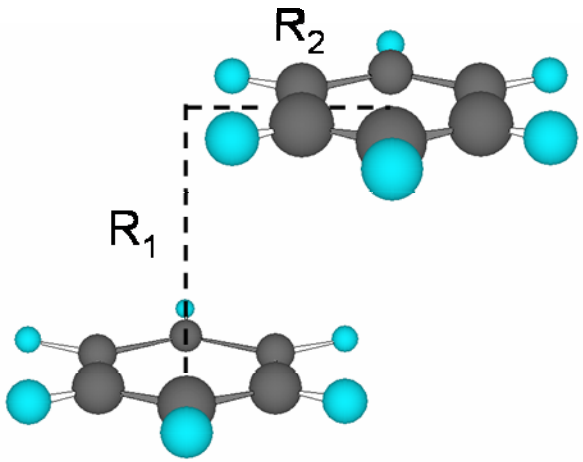

Slipped Parallel

The 75-point Euler-Maclaurin quadrature and the 302-point Gauss-Legendre quadrature are used for radial and angular grids, respectively.

Benzene dimer

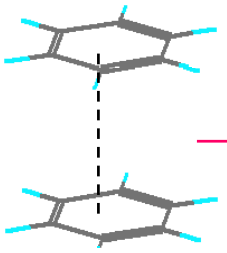

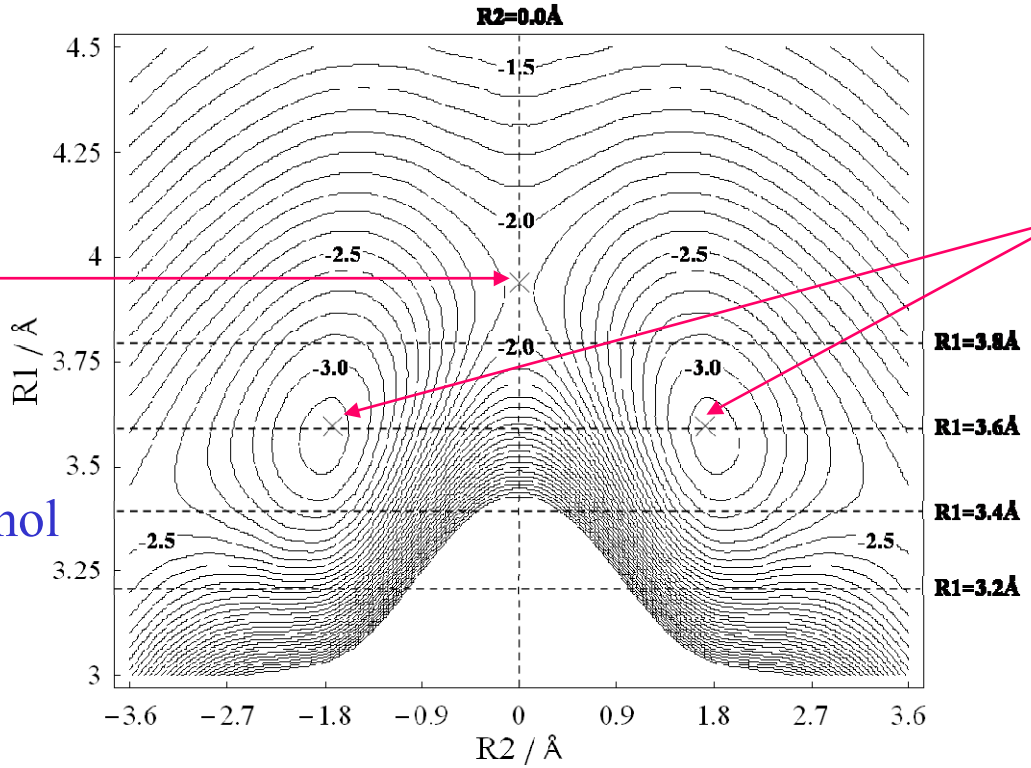

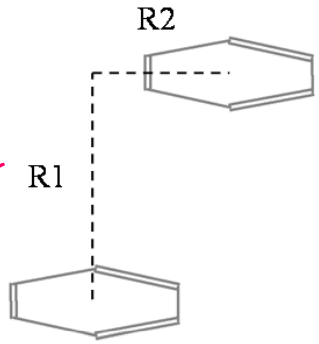

D_e=2.12 kcal/mol
R1=3.9 Å

Potential energy surface of benzene dimer

	D_e (kcal/mol)	R_1 (Å)	R_2 (Å)
Present/aug-cc-pVDZ	**3.17**	**3.6**	**1.7**
MP2/aug-cc-pVQZ	**4.79**	**3.4**	**1.6**
CCSD(T)/aug-cc-pVQZ	**2.63**	**3.6**	**1.6**

Naphthalene Dimer

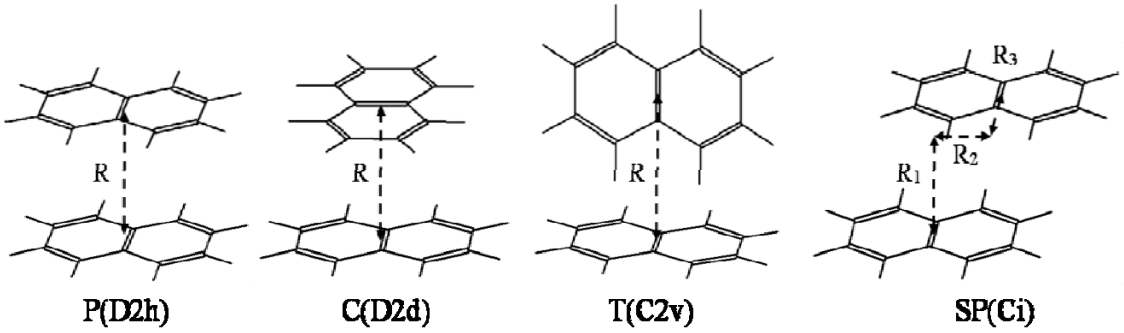

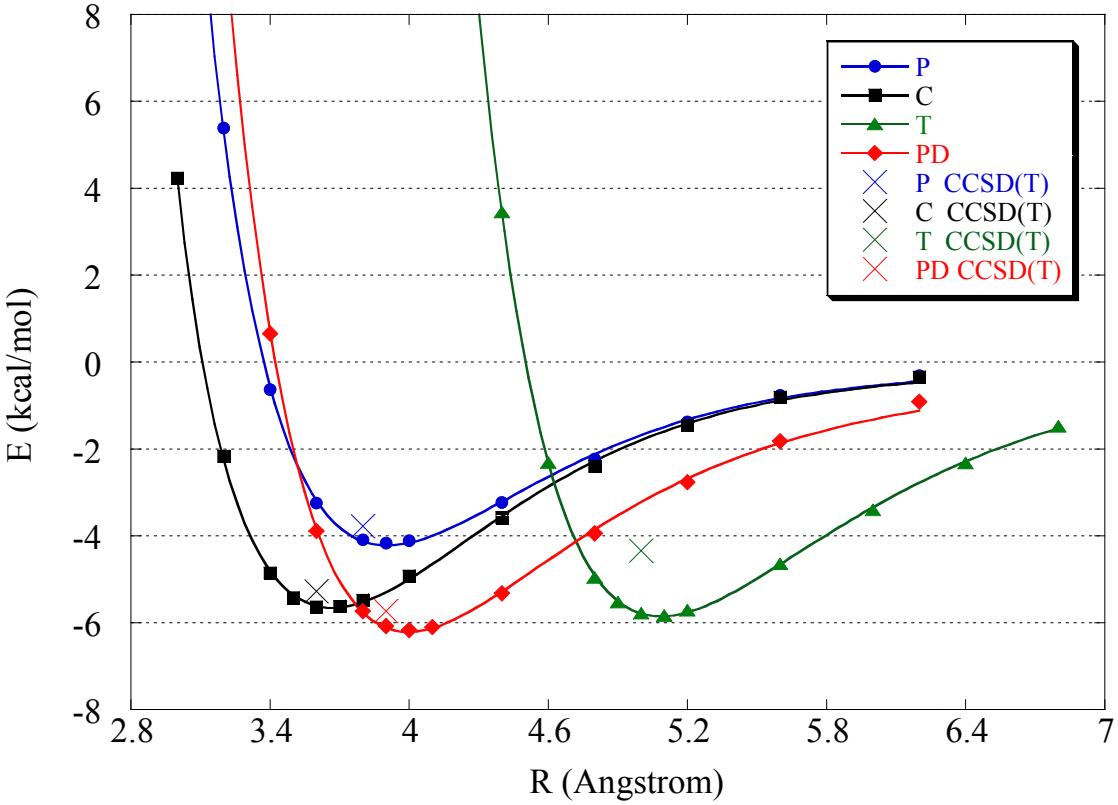

Our DFT 6.16 kcal/mol
CBS CCSD(T)
5.73 kcal/mol

Functional Dependence

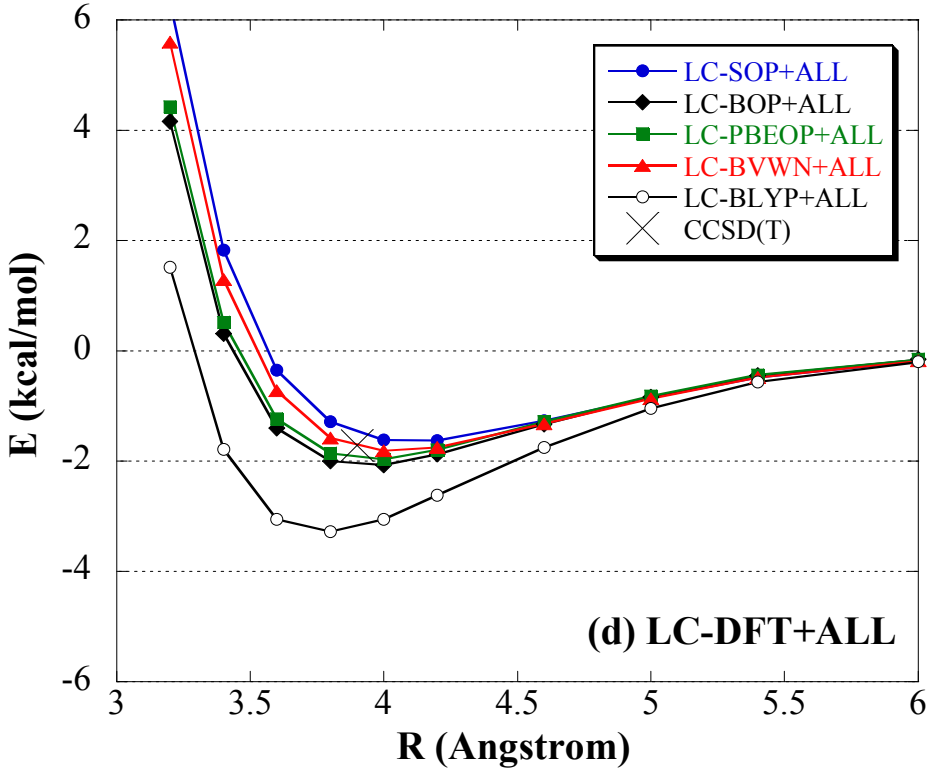

Parallel

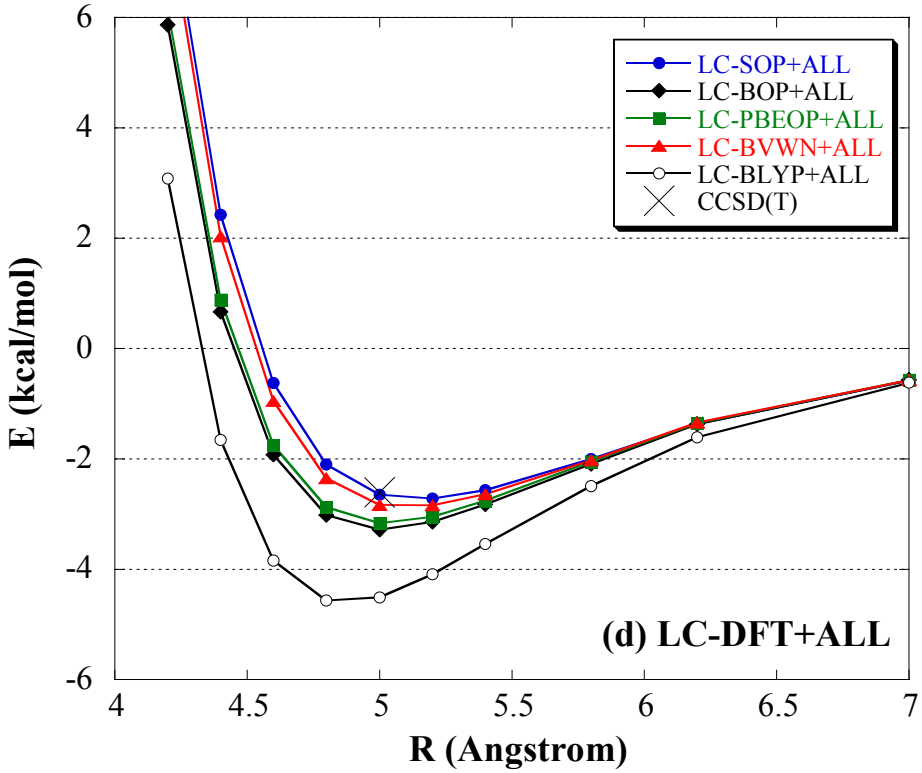

T-shape

BLYP functional gives substantially deeper potentials due to a different nature of the LYP correlation functional.

Basis set dependence

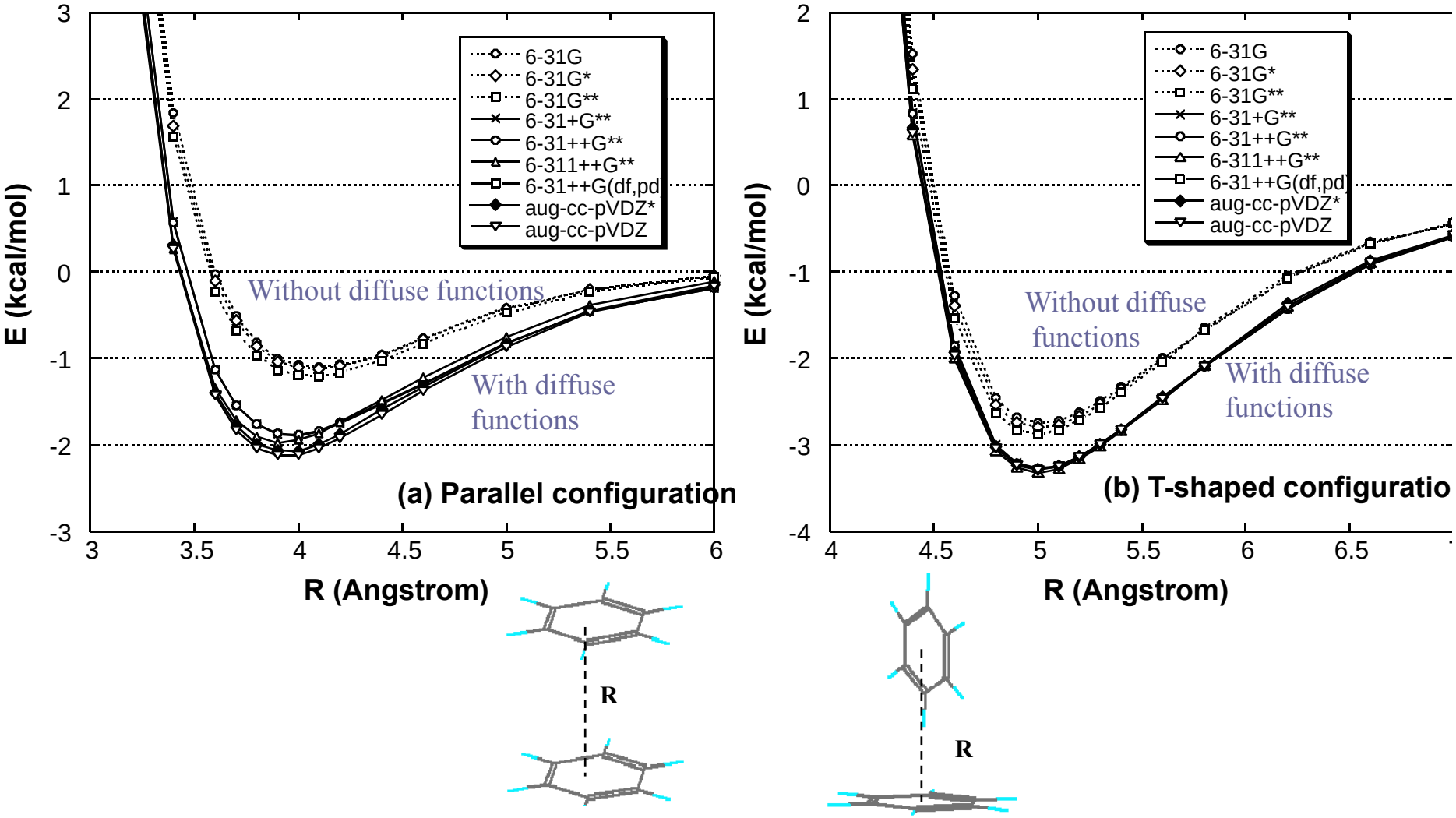

The calculated results have little dependence on the basis set used.

Structures of calculated complexes, with the point group symmetries and the definition of intermolecular distances.

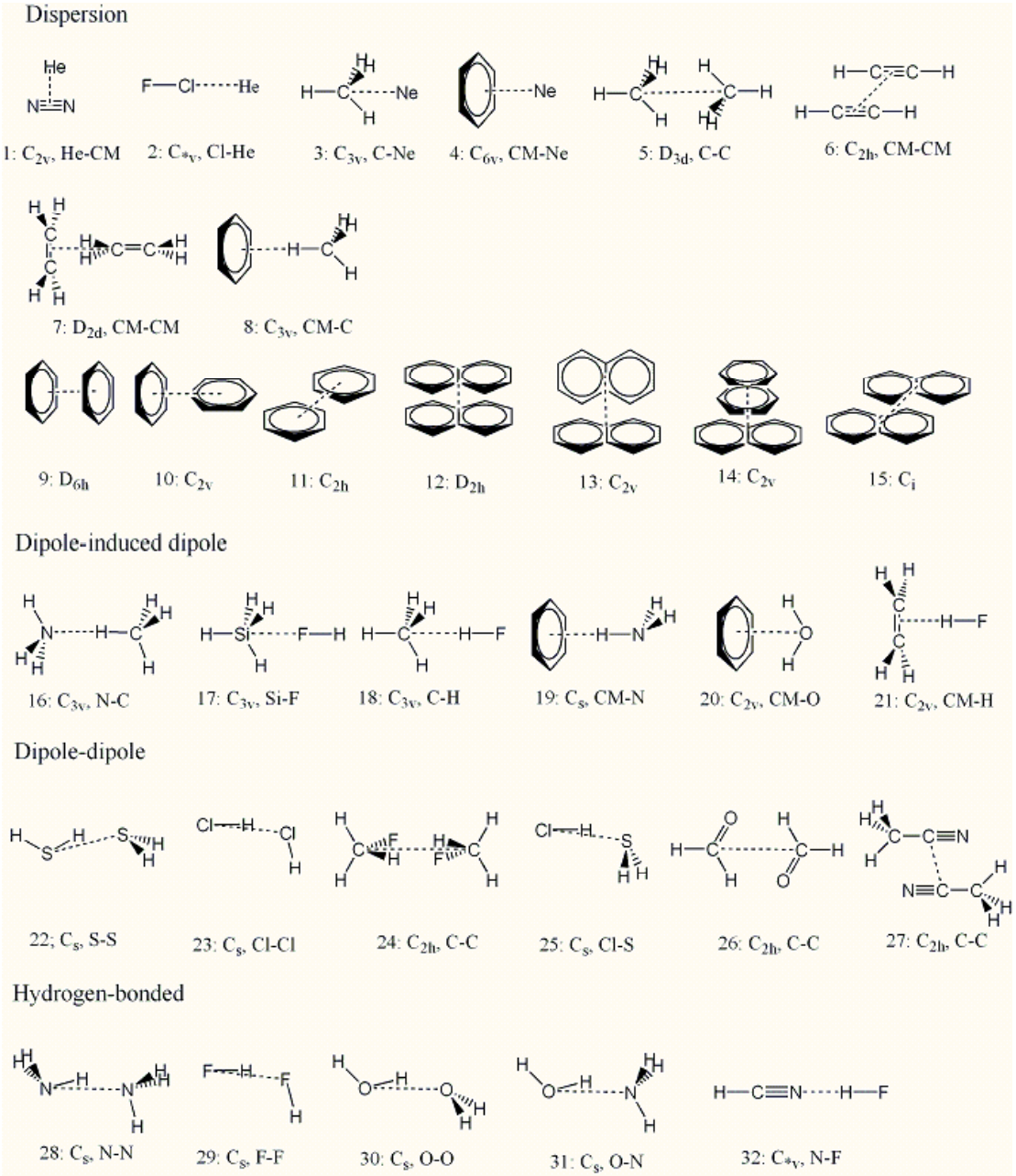

Mean absolute percentage error (%)

	Present	Becke	MP2
Binding energies			
Dispersion	9.9	14.9	46.6
Dipole-induced dipole	5.6	11.8	8.6
Dipole-Dipole	9.2	8.5	9.5
Hydrogen bonded	7.1	8.6	2.4
Overall	7.5	11.7	19.2
Separations			
Dispersion	0.11	0.08	
Dipole-induced dipole	0.08	0.02	
Dipole-Dipole	0.05	0.05	
Hydrogen bonded	0.06	0.08	
Overall	0.08	0.06	

Becke & Johnson, JCP (2005) : the model requires the polarizability of each monomer.

Application to π-stacking energies

- Large planar aromatic systems (graphene sheets, porphyrins, DNA bases) are attracted by a considerable dispersion force.
- The dimerization energy is difficult to measure because of decomposition
- In the limit of large parallel sheets, the dispersion force diminishes as $1/r^4$, not as $1/r^6$

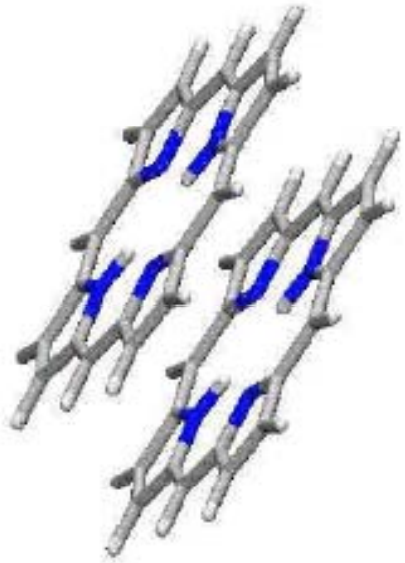

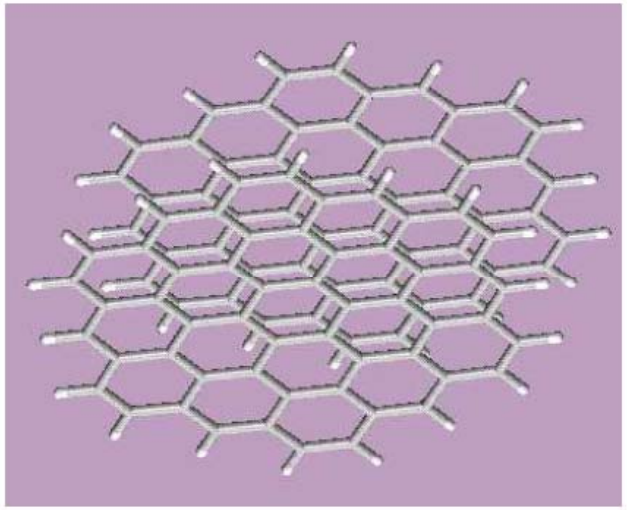

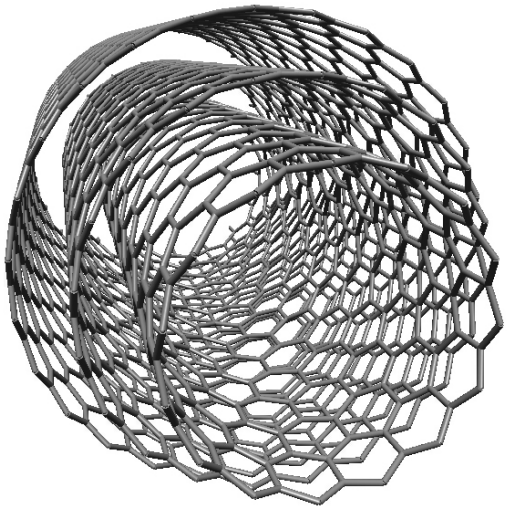

π-stacking energies

Coronene dimer ($C_{48}H_{24}$) & trimer ($C_{72}H_{36}$)

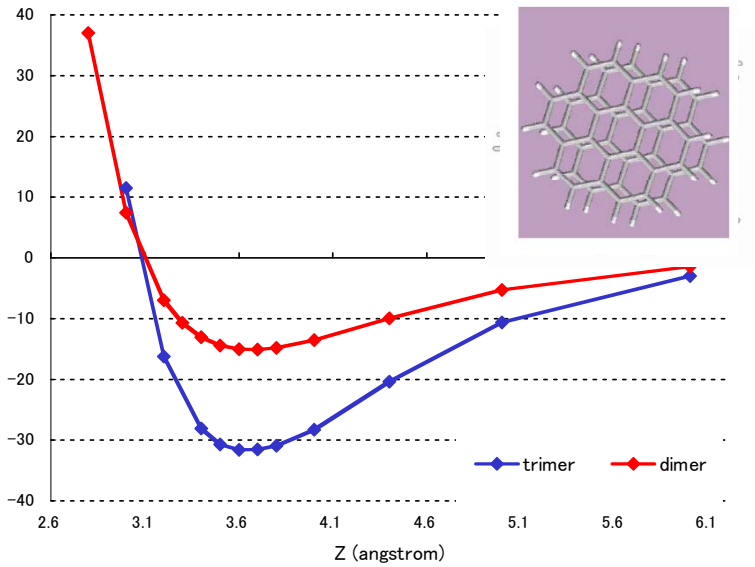

Circumcoronene dimer ($C_{108}H_{36}$) & trimer ($C_{162}H_{54}$)

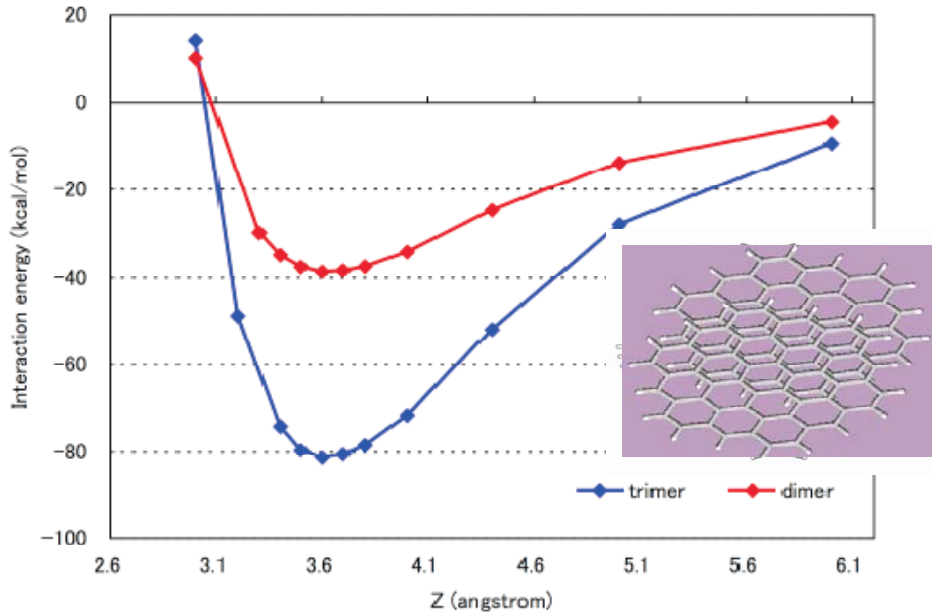

LC-BOP/ 6-31++G**

1008 BFs

z = 3.6 Å
15.0 kcal/mol
(MP2 35.0 kcal/mol)

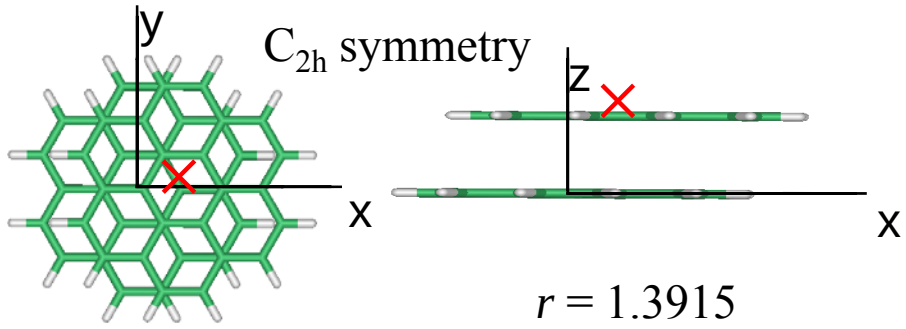

C_{2h} symmetry

r = 1.3915

2160 BFs

z = 3.6 Å
38.5 kcal/mol
(MP2 98.5 kcal/mol)

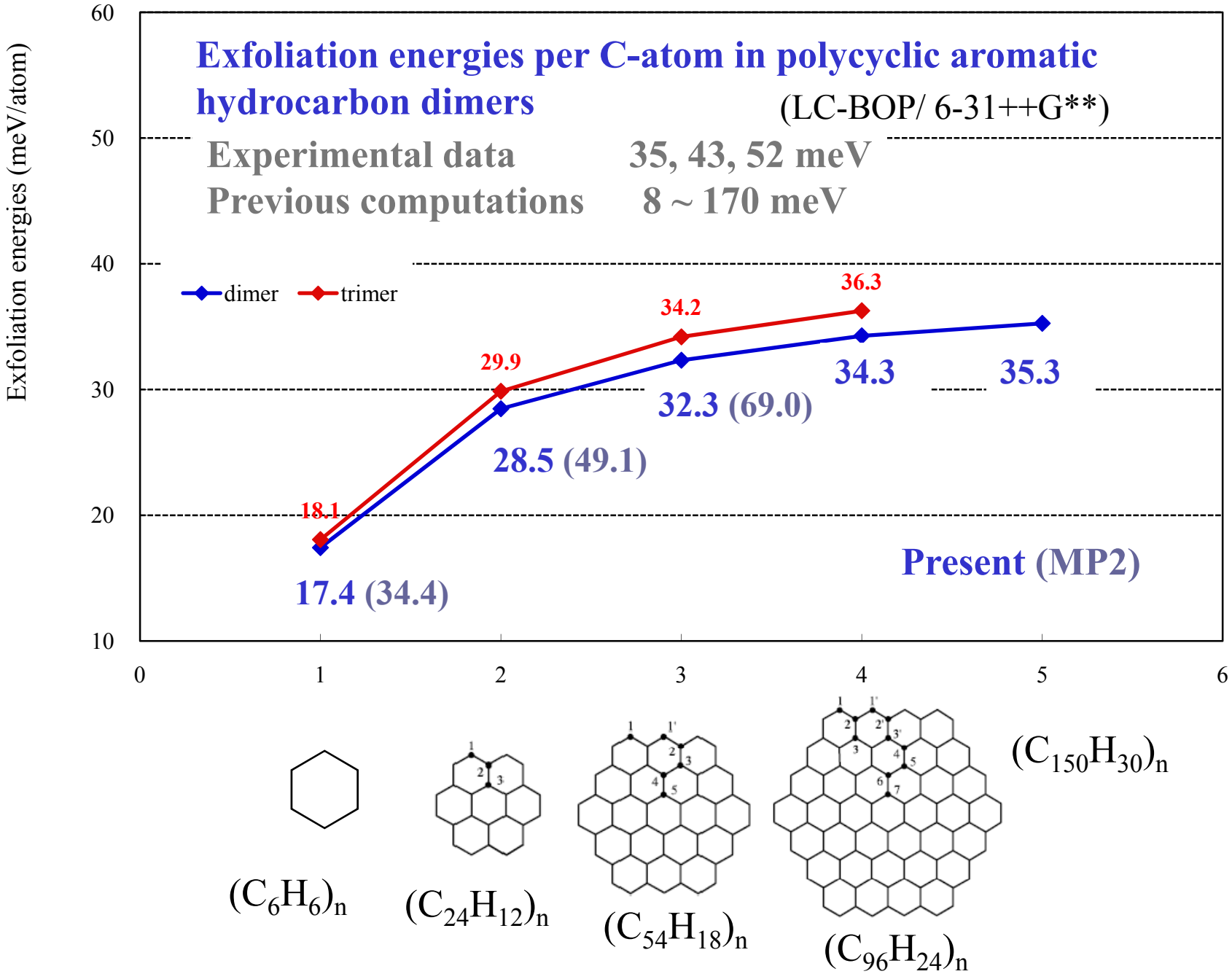
Exfoliation energies per C-atom in polycyclic aromatic hydrocarbon dimers
(LC-BOP/ 6-31++G**)
Experimental data 35, 43, 52 meV
Previous computations 8 ~ 170 meV
Exfoliation energies (meV/atom)
dimer
trimer
18.1
29.9
34.2
36.3
17.4 (34.4)
28.5 (49.1)
32.3 (69.0)
34.3
35.3
Present (MP2)
60
50
40
30
20
10
0
1
2
3
4
5
6
$(C_6H_6)_n$
$(C_{24}H_{12})_n$
$(C_{54}H_{18})_n$
$(C_{96}H_{24})_n$
$(C_{150}H_{30})_n$

Exfoliation energies per C-atom in polycyclic aromatic hydrocarbon dimers and trimers

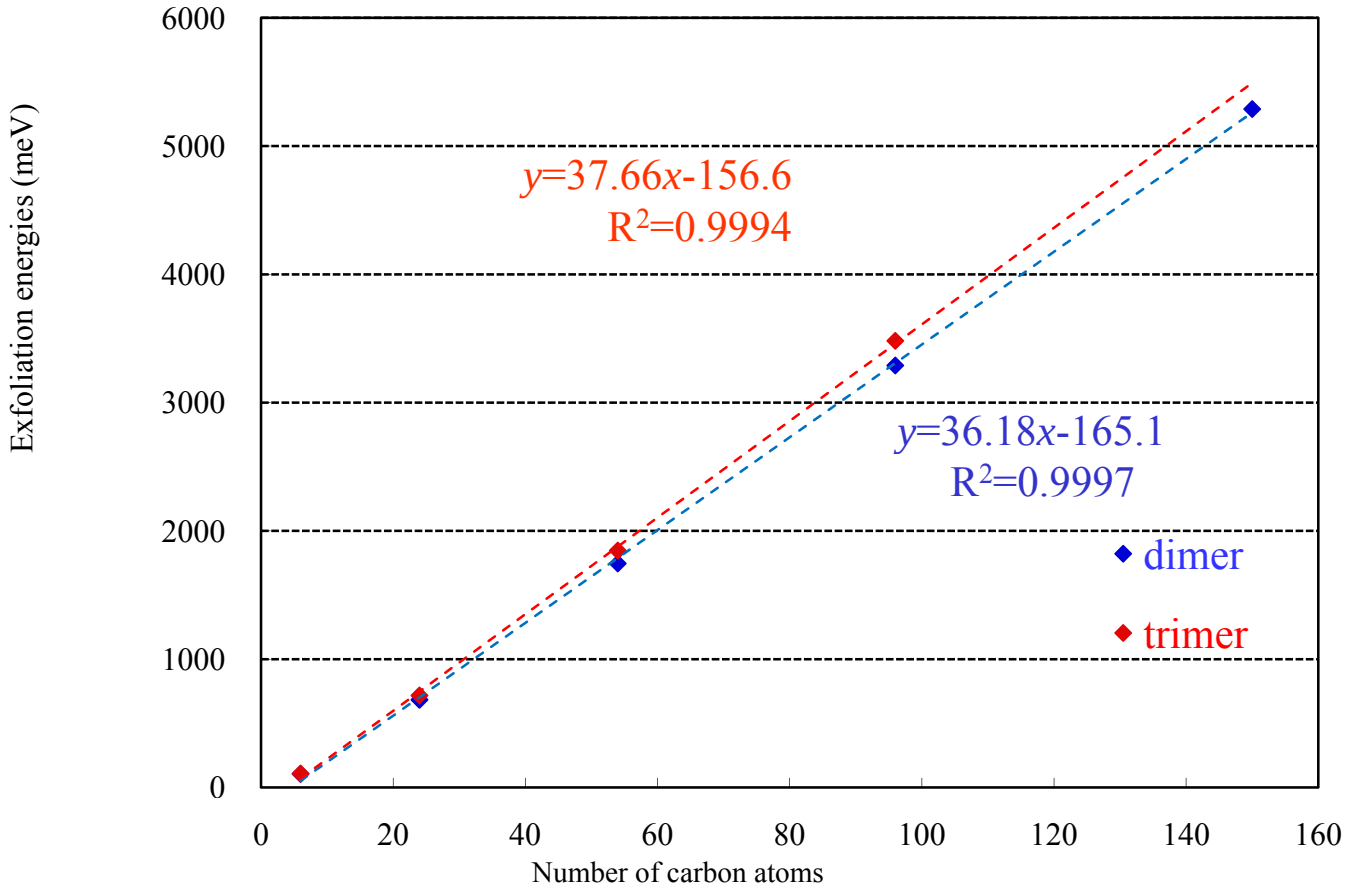

Experimental data	**35, 43, 52 meV**
Previous computations	**8 ~ 170 meV**
Present estimation	**36 ~ 38 meV**

Van der Waals Interactions

The proposed method is expected to be a promising alternative for calculating accurate van der Waals interactions in larger molecules, since this method requires much less computational cost compared to high-level *ab initio* wave function methods, such as CCSD(T).

Hirao Group (UT)

Thanks to Ministry of Education, Japan Science and Technology Agency (JST), past and present group, and many others.